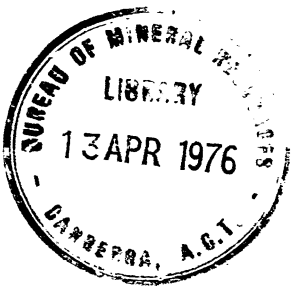

REPORT 176

Seismological Report on the Madang Earthquake of 31 October 1970 and Aftershocks

I. B. EVERINGHAM

DEPARTMENT OF MINERALS AND ENERGY
BUREAU OF MINERAL RESOURCES, GEOLOGY AND GEOPHYSICS

REPORT 176

Seismological Report on the Madang Earthquake of 31 October 1970 and Aftershocks

I. B. EVERINGHAM

AUSTRALIAN GOVERNMENT PUBLISHING SERVICE
CANBERRA 1975

DEPARTMENT OF MINERALS AND ENERGY

MINISTER: THE HON. R. F. X. CONNOR, M.P.

SECRETARY: SIR LENOX HEWITT, O.B.E.

BUREAU OF MINERAL RESOURCES, GEOLOGY AND GEOPHYSICS

ACTING DIRECTOR: L. C. NOAKES

ASSISTANT DIRECTOR, GEOPHYSICAL BRANCH: N. G. CHAMBERLAIN

Published for the Bureau of Mineral Resources, Geology and Geophysics by the Australian Government Publishing Service

ISBN 0 642 00987 2

MANUSCRIPT RECEIVED: JULY 1974

ISSUED: JANUARY 1975

Printed by Graphic Services Pty Ltd, 86a Pirie Street, Adelaide 5000

CONTENTS

TABLES

PLATES

FIGURES

SUMMARY

The most costly earthquake known in Papua New Guinea occurred near Madang on 31 October 1970. The adopted epicentre was 4.95°S, 145.68°E, the focal depth was 41 km, and the magnitude was 7.0.

The maximum intensity was at least MM8. Damage estimated at $1.7 million was caused by intensities of MM7 or more over an area of about 10 000 km^2, 15 lives were lost, a minor sea-wave was generated, and extensive landsliding occurred in the region of the epicentre. However, well designed buildings at Madang (MM7) were not damaged.

The aftershock pattern and first-motion data suggest that the earthquake was a result of near-vertical sinistral strike-slip faulting in the direction 069°.

Epicentres and magnitudes were determined for about 200 aftershocks which occurred during the four weeks after the main event. The magnitude/frequency relation for aftershocks was:

$$\log N = 4.71 - 0.73 \text{ MB (PMG)}$$

the b factor, 0.73, being markedly lower than for the regional and global seismicity, viz. 1.2.

INTRODUCTION

The subject of this report is the major earthquake that occurred close to Madang, on the northern coast of New Guinea, at 1743 Universal Time (UT) on 31 October 1970 (0343 a.m. local time on 1 November), and related events. Fifteen deaths occurred as a result of the earthquake, and damage was estimated at $1.7 million. Localities are shown in Figures 2, 3, 5, and 6.

Madang lies in a region of seismic activity extending along the northern part of the island of New Guinea and has often been shaken by earthquakes in the past. An idea of the seismicity of the area can be obtained from Figure 1, which shows the distribution of larger earthquakes in the Madang area since 1926. Here it may be seen that an earthquake with magnitude of at least M = 6.0 has occurred within about a 1° range of Madang about every three years. Fortunately many of the earthquakes in the region are at depths greater than 100 km, and the peak intensities resulting from such earthquakes are usually not high enough (MM greater than 7) to cause notable damage. Brooks (1965) estimated the return period for an MM8 intensity in the Madang region to be of the order of 40 years.

That Madang had been shaken by an early-morning earthquake was first reported to Port Moresby Observatory by the Director of Civil Defence on Sunday 1 November 1970, at about 0800 EST. After reading the seismogram to locate the epicentre and measure the magnitude it was decided that the event was large enough to warrant field seismic recordings and inspection of damage.

Two seismographs and two observatory staff members were transported by charter plane to Madang on the afternoon of 1 November, and a seismograph started recordings at Madang at 8 p.m. (just over 16 hours after the main event). This seismograph operated almost continuously until 28 November.

During the four days (2-5 November) immediately after the earthquake, observatory staff investigated and photographed the earthquake effects in the Madang area and gave advice on earthquakes. Trouble with a Willmore seismograph spoilt all but a few hours of field recordings attempted at sites north of Madang. However, the instrument was later operated successfully by observatory staff for a week (18-24 November) north of Madang at the nearest accessible point to the epicentral region of the aftershocks. The Rabaul Volcanological Observatory staff installed a temporary station at Karkar Island for the period 1-13 November. Details of the recording stations are given in Table 1.

TABLE 1. DETAILS OF SEISMOGRAPH STATIONS

Station	*Code*	*Latitude °S*	*Longitude °E*	*Elevation (metres)*
Port Moresby	PMG	9.409	147.153	67
Lae	LAT	6.653	147.000	72
Rabaul	RAB	4.192	152.171	184
Esa'ala	ESA	9.738	150.814	46
Tabele	TBL	4.101	145.011	180
Wabag	WAB	5.494	143.728	2032
Momote	MOM	2.074	147.411	10
Goroka	GKA	6.058	145.391	1634
*Madang	MAD	5.230	145.793	3
*Sumerang River	SUM	4.918	145.775	3
*Karkar	KAR	4.563	145.925	3
*Plantation Hotel	PLN	4.950	145.775	3

* Temporary station

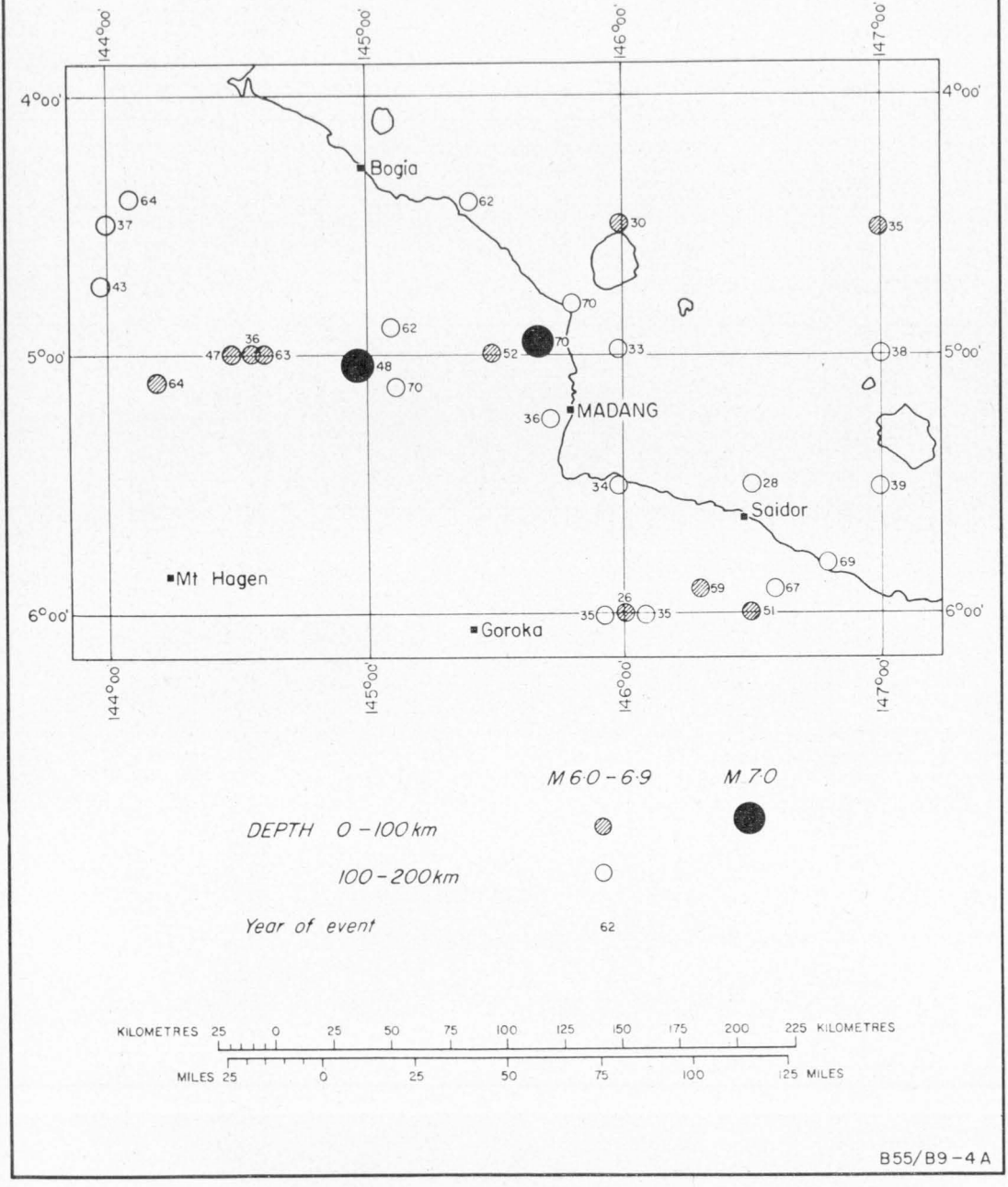

Fig. 1. Earthquakes in the Madang area with magnitudes 6.0 or greater, 1926-1970.

EARTHQUAKES

TABLE 2 — EVALUATION OF INTENSITY

EFFECT	M.M. INTENSITY					
	III	IV	V	VI	VII	VIII
GROUND MOVEMENTS	Faint Felt by half population.	Moderate Felt by most.	Strong Felt by all.	Very strong Slightly affects walking.	Difficult to stand.	People thrown down.
SEEN/HEARD (other sounds apart from rumbling)	Faint rattle of windows, house creaks. Hanging objects swing slightly.	Windows, crockery, etc., rattle, building creaks. Trees shake slightly. Slight sloshing of tank water.	Unstable objects move. Pictures swing. Tree movements obvious. Water sloshes in tanks.	Objects fall, furniture moves. Trees strongly shaken. Water sloshes out from tanks.	Ground waves. Water waves.	Odd trees fall.
AWAKENED	Few	Many	All except few heavy sleepers.	All	All	All
ALARMED	Nil	Very few alarmed.	Few alarmed.	Many alarmed, run out of doors.	All alarmed.	Some terrified.
DAMAGE	Nil	Nil	Weaker water tanks leak.	Few water tanks burst. Obvious cracks in weak masonry. A few weak village huts collapse.	Many burst tanks. Unreinforced brick walls collapse. Weaker village huts collapse. Minor damage to house stumps.	Timber framed huts and houses off stumps. Roughly half, village huts off stumps or thrown down.
SLUMPING and LANDSLIDES		Rare landslides.	Occasional landslides	Occasional landslides	A few landslides. Settlement and cracking of unconsolidated ground.	Extensive landslides. Bad slumping of built up areas. Reef settlement.

Port Moresby Geophysical Observatory,
Box 323, Post Office, Port Moresby,
Papua New Guinea.

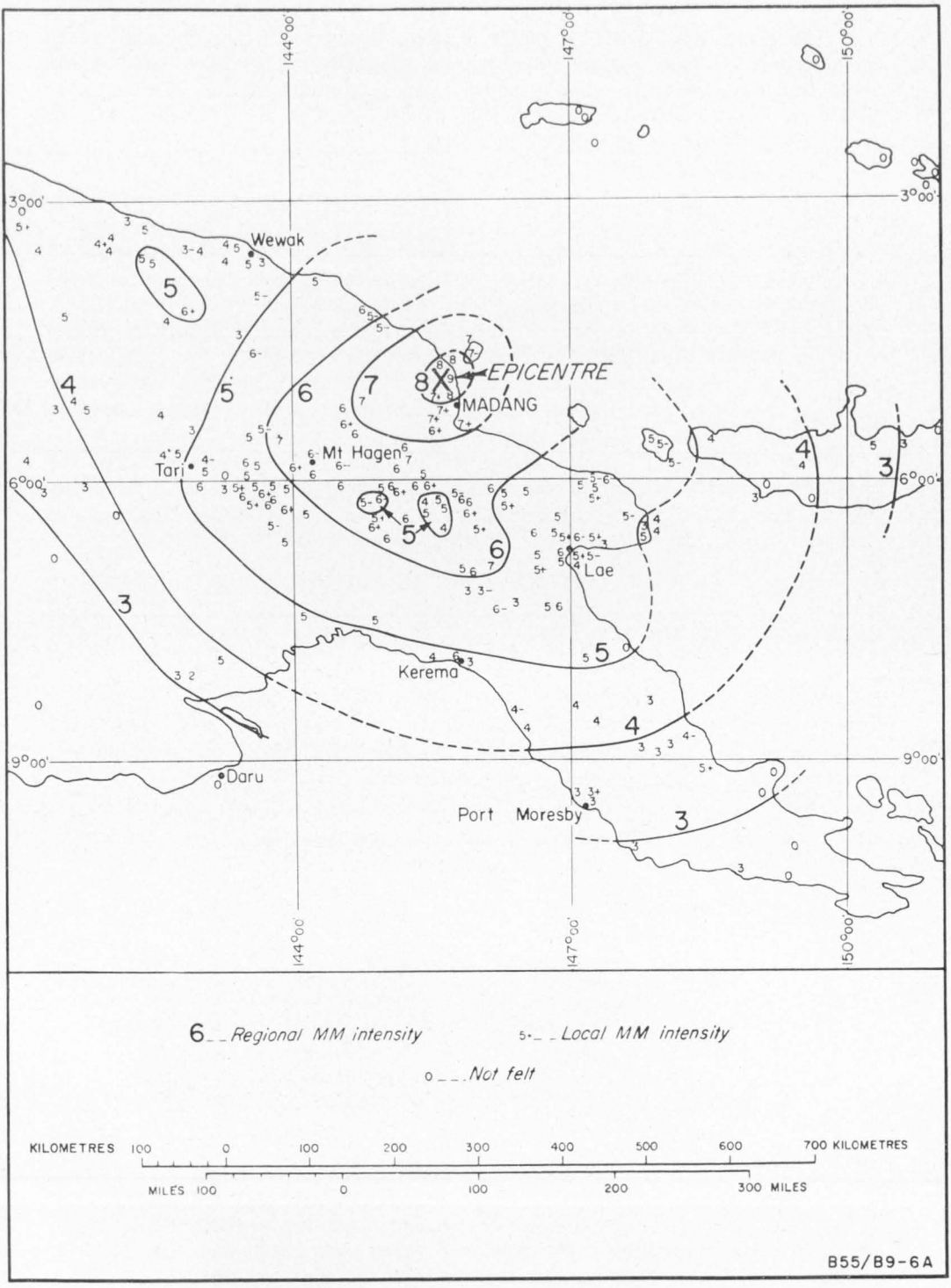

Fig. 2. Isoseismal map for the Madang earthquake, 31 October 1970.

This report gives a brief coverage of seismological features of the earthquake and aftershock series. Further investigations should follow as time permits, and some conclusions given here may be changed as a result. Details of damage to buildings, bridges, wharfs, and other structures are not given as they will be discussed elsewhere by appropriate authorities.

EARTHQUAKE INTENSITIES AND DAMAGE

Figure 2 shows the isoseismal map, information for which was obtained from 220 intensity questionnaire replies and from aerial and ground inspection near the epicentre. The intensities assigned in Figure 2 are based only on the questionnaire replies. The chart shown in Table 2 was designed to maintain uniformity of assessment of intensity using the more common evidence available in the Territory; a general idea of the effects of the earthquake at different intensity levels may be gathered from this chart. Typical damage effects are illustrated by photographs in Plates 1 to 7. Details of damage have been given by Baker (1970), Berg (1970), Duncan & Hollings (1970), and Hill (1970), and have been summarized by the Papua New Guinea Advisory Committee on Seismology and Earthquake Engineering (ACSEE, 1973). Hogg & Robertson (1971) discuss some sociological aspects.

TABLE 3. DEATHS CAUSED BY THE MADANG EARTHQUAKE

Place	*Remarks*
ASIWO	2 girls and 1 boy buried by landslide
SUMERANG RIVER	1 boy lost from fishing boat off mouth of Sumerang River when swamped by waves caused by earthquake
BUNU	1 man killed by collapsed copra drier
GUHUP	1 woman killed by collapsed house
HILU	1 woman and 1 girl killed by collapsed house
CHUAVE AREA (6°07′S, 145°08′E)	1 girl killed by collapsed house
LUFA AREA (6°12′S, 145°09′E)	3 women and 3 girls buried by landslide

A list of deaths and an estimate of the damage, based mainly on information given by the District Commissioner for the Madang District (Clifton-Bassett, 1970), are presented in Tables 3 and 4. Damage to buildings was around $660 000; to roads, wharves, and bridges $270 000; and for repairs to the SEACOM cables $550 000. The cost of replacing 847 village houses destroyed by the earthquake will be about $100 000 allowing for salvaged materials.

The earthquake was felt throughout the eastern half of the island of New Guinea and in western New Britain. The region of greatest shaking was near the epicentre, where intensities of MM8 or more were experienced (see Fig. 3). It is not possible to assess the maximum intensity with any confidence because evidence from standard intensity scale data was not available, the area being relatively

uninhabited. Generally the intensity of MM8 or more was apparent from the facts that people fell over and about fifty percent of village houses (made from timber, bamboo, and grass, and mounted on stilts about one metre high) were badly damaged. Landslides (described by Pain, 1972) were very common in the mountainous area of the Adelbert Range (Fig. 3; Plate 1), which lies in the central part of the region experiencing intensities MM8 or greater, and intensities around MM9 probably occurred here. Landslide evidence noted from the air was used exclusively to determine the western part of the MM8 isoseismal.

In this area of greatest intensity, bridges moved and their built-up approaches slumped badly (Plates 3 and 4). Six deaths resulted from landslides or collapse of village houses (Plates 2 and 3), and a few trees were shaken down.

TABLE 4. DAMAGE — SUMMARY OF COSTS

Details	*Estimated Value*	
Administration property	$	$
—Architectural	191 100	
—Roads and bridges	100 000	
		291 100
Commonwealth instrumentalities		
—Architectural	5 250	
—Stores and equipment	300	
—Water tanks	10 200	
—Other (incl. SEACOM Cable)	550 000	
		565 750
Local govt councils		
—Council administration	1 950	
—Health facilities	6 270	
—Water supply	2 050	
—Roads and bridges	2 000	
		12 270
Madang town area—private firms		
—Architectural premises	257 184	
—Architectural residences	37 845	
—Water tanks	36 248	
—Stocks and equipment	62 235	
		393 512
Private plantations		
—Building and plant	26 420	
—Water tanks	1 030	
		27 450
Mission stations		
—Architectural	57 000	
—Water tanks	2 420	
—Education buildings	29 620	
—Wharves	172 000	
—Roads	500	
—Other	900	
		262 440
Villages		
—Houses (847)	97 405	
—Fishing boat	4 000	
		101 405
TOTAL ESTIMATED COST		$1 653 927

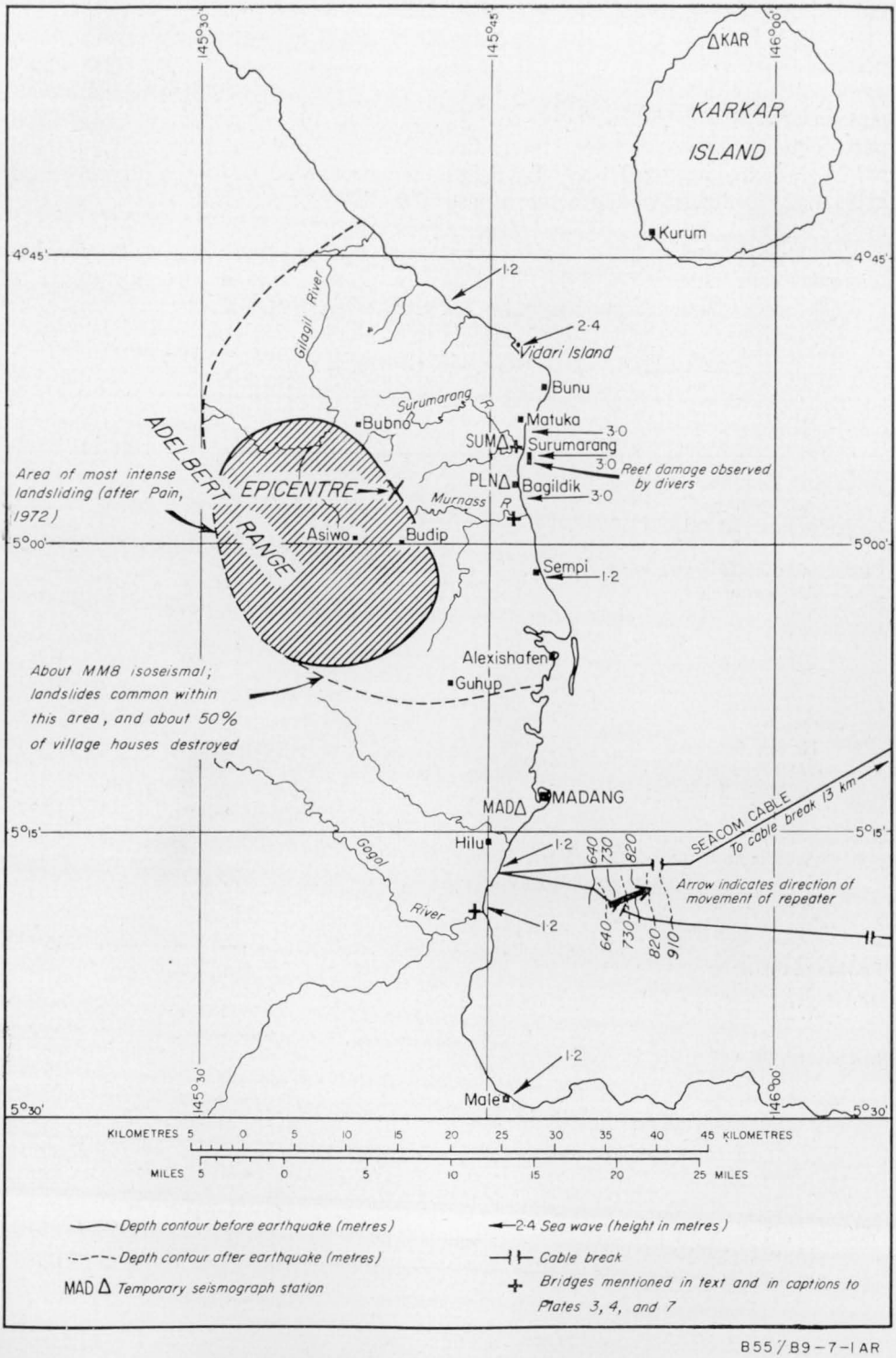

B55/B9-7-1AR

Fig. 3. Earthquake effects in the epicentral region.

PLATE 1.

(a) Typical landslide, Adelbert Range. Fallen timber eventually found its way to the river mouths and caused large log jams.

(b) Landslides around wrecked village, Adelbert Range. Note how the slope in the foreground was just on the point of sliding as evidenced by ground cracks at the top of the slope below the village.

(a) Lightfoot Arcade, Madang. Note that the wall has fallen outwards, and the roof is held up by shelving in the centre of the photograph.

(b) East-west tension feature (about 100 m long) caused by large-scale slumping of ground parallel to the river at left (outside photograph), near Sempi village.

PLATE 3.

(a) Typical village wrecked by earthquake. About 50 percent of houses were wrecked where intensity was MM8 or more.

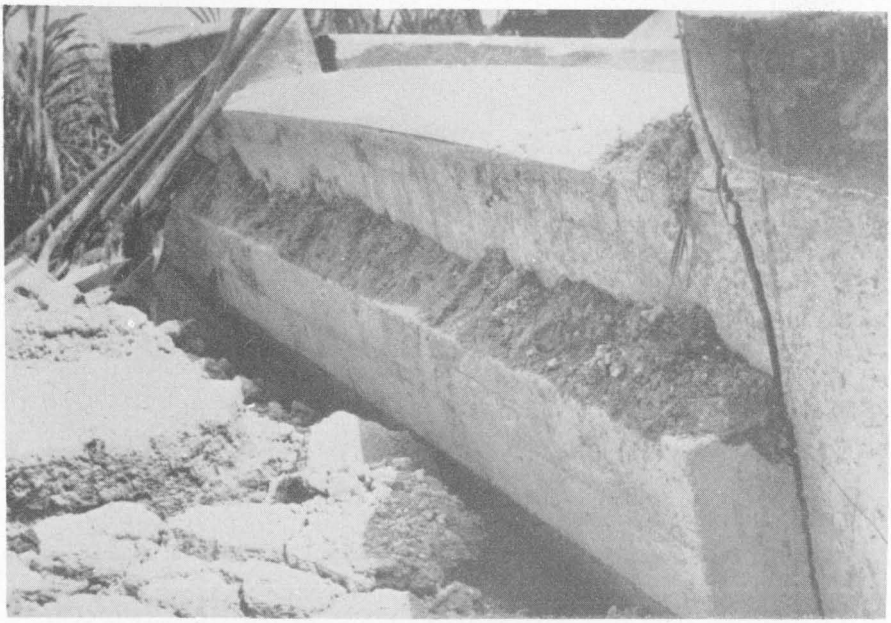

(b) Surumarang River bridge thrust against northern abutment. Note the settling of the built-up approach (left) previously level with the top of the abutment. The bridge runs transversely to the direction of the epicentre.

PLATE 4.

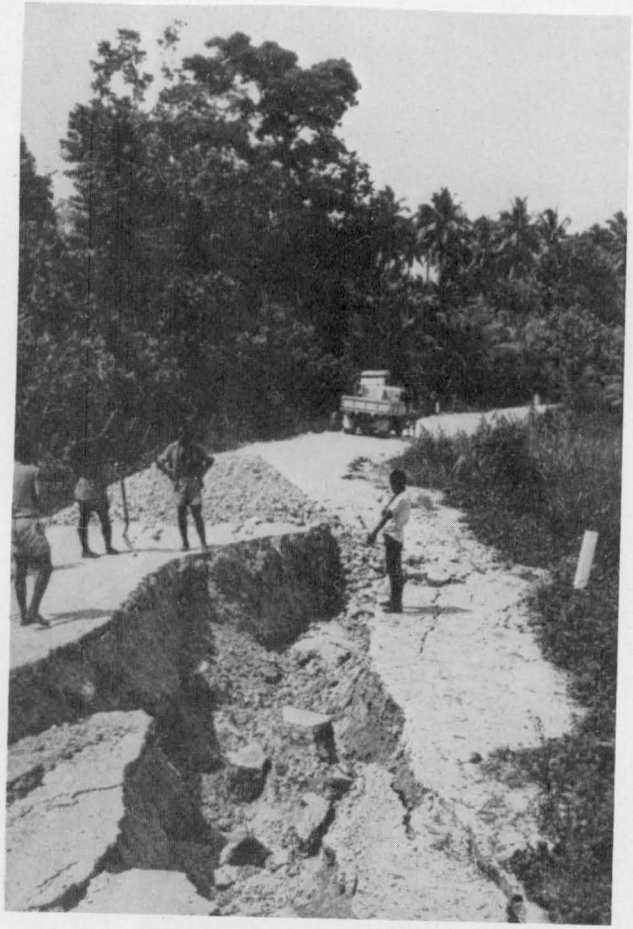

(a) Slumping and settling of the Surumarang River bridge approach — typical outcome of built-up sections of roads near bridges where MM7 or greater intensity occurred. The six-metre-high built-up approaches to the Gogol River bridge settled two metres.

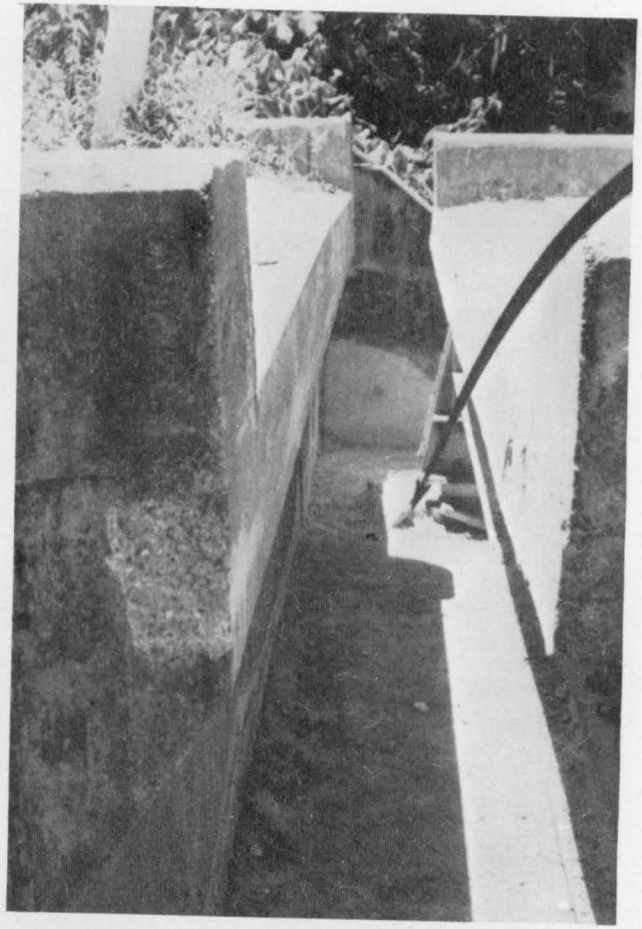

(b) Surumarang River bridge moved 33 cm north-northwest away from the southern abutment (at left of photograph). Note sheared holding-down bolts (2.2 cm diameter).

In the area with intensities MM7 to MM8, landslides were common in hilly terrain, but much less so than within the MM8 isoseismal. People experienced difficulty in standing and some bridge approaches slumped. The latter effect resulted in abutment failure at the Murnass River (Plate 7). Unreinforced brick and concrete-masonry buildings (Plate 2) and weaker village houses (Plate 3) were badly damaged, and roughly one-third to one-half of the water tanks (circular, galvanized, corrugated iron) were damaged (Plate 7). However, timber homes on high foundation piers, and well built brick buildings, were unscathed. The piers supporting the main concrete wharf at Madang were damaged at the junction of the shorter (landward) piles with the pile caps (Plate 5), and a large steel-framed storage shed on the wharf suffered substantial damage to the bracing system and internal lining.

Earthquake-induced sea waves (tsunamis), submarine slides, and reef damage (effects are described later) were noted in the areas with intensities MM7 or greater (Fig. 2). The Overseas Telecommunications Commission's SEACOM cables were broken at several points by slides off the coast near Madang.

In areas farther from the epicentre where intensities were less than MM7 some landslides did occur, but they were rare and whether or not sliding occurred depended mainly on the rainfall preceding the shaking. Six persons were killed by a landslide near Lufa, and another by a slide near Chuave. Both villages are about 120 km south of the epicentre.

An interesting after-effect of the earthquake was the river transportation of vast quantities of timber from the landslide regions to the sea. Log jams formed at bridges over the Sumerang* and Gilagil Rivers near their mouths, and large logs in the coastal waters were a menace to small shipping. It would be interesting to discover where these logs, some of them about one metre in diameter, finally came to rest. Sieberg (1910) commented on the enormous quantities of timber carried into the sea as a result of the major earthquake of 12 September 1906 at 7°S, 149°E.

Evidence from an observer at Vidari Island (Fig. 3) during the earthquake suggested that the island subsided about one metre (see next section). A similar effect was found by J. Bowler (pers. comm.) of the Australian National University, Canberra, at an area on the mainland a few kilometres from Vidari Island. Here local subsidence had occurred, bringing the bases of coconut palms on a grassy terrace below the level of high tide. Along part of the Madang harbour, 20 cm subsidence was reported by the harbour authorities.

R. A. Davies, of the Papua New Guinea Geological Survey, also noted subsidences on the west coast of the volcanic island of Karkar. For example, he stated (pers. comm.) that at Kurum village:

> 'Flooding seems to suggest that the coastline has subsided over 0.3 metres, for a distance of several hundred metres. The sea water in this area was charged with mud for a period of several days following the earthquake. The reef seems to be unaffected.'

and at Kurum Plantation:

> 'A circular collapse feature, some 10 metres diameter, was found after the earthquake. A coconut palm, approximately 20 metres in length, had dropped

---

* The official name of the village and river is Surumarang; however, local and unofficial usage by Government officers is 'Sumerang', and this will be used throughout the text of this report.

(a) Floor and stilt structure of village house. Note that the stilts are not tied to the flooring, nor are they braced. The stilts sag north-northeast, transverse to the direction of the epicentre.

(b) Madang wharf damage. Concrete spalled by plastic hingeing at the top of the short piers at the landward side of the wharf.

(a) Madang wharf movement. Relative movement of about 8 cm between the mainland and Madang main wharf (at right) is evidenced by bitumen scraped off the wharf by the steel plate joined to the mainland.

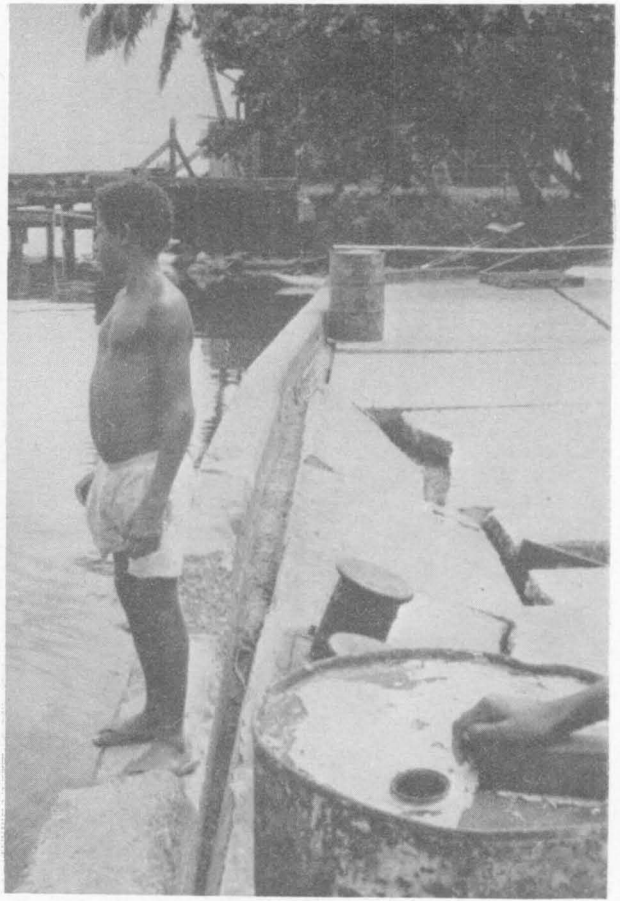

(b) Small-ships wharf, Madang. Sheet piling has moved outwards and back-filling has subsided causing deck slab to settle and fracture.

(a) Failure of abutment, Murnass River bridge — typical failure of smaller bridges.

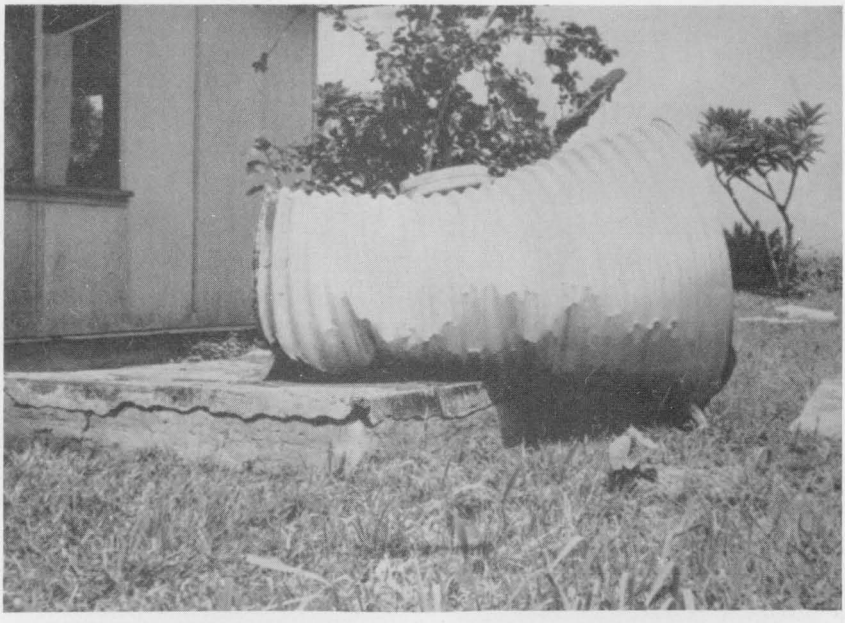

(b) Wrecked tank, Talidik. Tanks burst in numerous ways, which appeared to be caused by the resonant effects of water in a weak container.

vertically into the hole, such that only the terminal fronds are now visible, and these are immersed in water some 3 metres below normal ground level.

'Other areas of subsidence are common and some buildings were tilted during the earthquake. The subsidence can probably be explained in terms of underground water, as, in many areas on Karkar, surface runoff gives way to subterranean migration. This migration is probably responsible for the solutioning and removal of buried volcanic tephra.'

Regional changes in elevation were not noted and the cause of the local subsidences is believed to be settlement of poorly consolidated sediments beneath the coastal regions.

A strong-motion recording was made on an M02 accelerograph at Yonki, about 150 km south-southwest of the epicentre. Here the maximum ground acceleration was 0.1g and the local intensity MM6.

TSUNAMI AND SUBMARINE EFFECTS

Along the coast between 4°45′S and 5°30′S there was evidence of ocean waves resulting from the earthquake. The location and apparent height of the waves is shown in Figure 3. The coast was not systematically examined, and only places where the roads were close to the sea were visited. At most places it was impossible to make accurate measurements of the wave heights because the strand lines were not clear and the few eye-witnesses, having been awakened in the darkness by an earthquake, were extremely vague as to what they saw. Madang harbour was not equipped with a tide gauge, but harbour authorities stated that the tide was low. Normal tidal variation is about one metre.

At Vidari Island, an islet less than 1 km offshore, two independent observers stated that the ocean first receded. However, they disagreed on what happened subsequently. One witness reported a 2.3-m wave which persisted for several minutes. The other witness noted that after about 3 minutes the water had risen about one metre above its usual level and stayed there, i.e. the ground level apparently subsided.

In the V-shaped mouth of the Sumerang River, waves had lifted flotsam about 3 m above average high-tide level, and a fishing boat was swamped (with one fatality) by a turbulent sea offshore, not far from the river mouth. Possibly either *seiches* or relatively short-period waves generated by the movement of the reef caused turbulence. Such waves would appear more like normal ocean waves, as distinct from tsunamis, which have a longer period (see later discussion on sea waves at Suva).

The cause of the tsunamis is believed to have been submarine slumping (embryo turbidity currents perhaps), which occurred along the coast in the Madang region. Krause (1965) noted that the steep scarp fronting the reef slopes as much as 45° and extends to below a depth of 200 metres in some areas, so submarine slides would be easily triggered here. Divers also found extensive reef damage near the mouth of the Sumerang River and offshore from Madang. Large masses of coral were broken off, and many had slid down the steep slopes seaward of the reef (J. Bowler, pers. comm.; Stoddart, 1972).

The Overseas Telecommunication Commission's SEACOM cables (Fig. 3) to Guam and Cairns were each broken in two places. About 15 km east of the mouth of Gogol River, where the sea-floor has a slope of about 1:20, bathymetric contours

were displaced about 1 km to the east (i.e. the sea-floor became shallower by about 45 metres). A cable repeater unit was moved about 4 km east-northeast and buried, and both cables were broken.

The cable to Cairns parted about seven minutes after the earthquake started. Assuming that the slumping commenced in the area of the cable break, the cable could have parted after the repeater had been moved any distance up to 4 km, which indicates a maximum velocity for the slumping of about 34 km per hour. Slumping of loosely consolidated sediment dumped by the Gogol River would have been easily triggered in the area west of these breaks. Several kilometres downslope, where the sediments apparently came to rest (possibly where the gradient decreased slightly), the sea-floor rose as observed by the Overseas Telecommunications Commission. Landwards, at the source of slumping, where the material was removed, an increase in depth should have resulted.

Alternatively, if it is assumed that the slide started closer to the shore on that part of the sea-floor which slopes steeply from the seaward side of the reef down to depths of about 200 metres, a slide velocity of about 130 km per hour would be required for this slide to break the cable after seven minutes. There is no previous evidence to support such a high slide velocity (Menard, 1964), so it seems more likely that the slumping which broke the cable occurred in an area near the cable break.

Previous cable breaks (1966, 1968) in the Vitiaz Straits, described by Krause, White, Piper & Heezen (1970), were considered to have been caused by turbidity currents originating off the Markham River mouth and travelling at an average of 50 km/h (1966) and 3 km/h (1968) into the New Britain Trench. The cable breaks farther from the coast off Madang suggest that turbidity currents were also caused by the Madang earthquake.

All the types of marine effects noted near Madang and described above were observed with much greater clarity in Suva during an earthquake on 14 September 1953. Houtz (1962) made the following summary of effects there:

> 'Arrival times of the ensuing tsunami at various points were reconciled to show that the tsunami had an extended source from Suva harbor to Beqa island. The tsunami was clearly caused by the slumping of marine sediments immediately after the earthquake. The direct action of the earthquake produced small waves that served as warnings on Beqa and Kadavu islands. These waves are presumed to have been created by the vibration of the reef against the water. The destructive waves, arriving later, were produced by slumping effects originating on the edge of the marginal shelf. Their observed arrivals are consistent with this mechanism.
>
> 'The bathymetry of the affected area was resurveyed and bottom changes up to 300 feet vertically were found. At a distance of more than 30 miles from the slumps, submarine cables were disrupted and displaced by as much as 13 000 feet. It is inferred that these effects were caused by turbidity currents travelling down a gradient of about 5 percent for the first 10 miles and nearly flat thereafter.'

A catalogue of New Guinea/Solomon Islands tsunamis (Everingham, in prep. a) indicates that waves up to 3 m in height, similar to those generated by the Madang earthquake, are not uncommon in New Guinea and could be expected every few years on average.

ERRATUM FOR REPORT 176 - p. 18, paragraph 3, line 4: 3 km/hr read 30 km/hr.

THE MAIN EARTHQUAKE, FORESHOCKS, AND AFTERSHOCKS

The main earthquake

With the exception of Lae (LAT) all permanent stations (see Table 1) in the Papua New Guinea network recorded a P time for the event. The S time was recorded only at Port Moresby (PMG) on the very-low-gain seismograph because at all other stations the recordings were off-scale at the time of the arrival of the S wave. ML was determined approximately from the PMG and Rabaul (RAB) Wood-Anderson seismographs by extrapolating the coda of recorded S waves to the point where a maximum deflection was estimated to be.

Three values of the hypocentre and the origin time were determined: by the US National Ocean Survey (NOS — previously CGS) using data from 100 international stations; by the Port Moresby Observatory using the computer program HYPO (James, Sacks, Lazo & Aparicio, 1969) and data from seven stations of the local network; and by BMR Canberra using a Lamont program based on Bolt's (1965) program and mainly southern hemisphere data (25 stations). Results of these determinations along with magnitudes are:

Source	*H (UT) 31 Oct. 1970*	*Epicentre Lat. °S*	*Long. °E*	*Depth km*	*Mag.*
(a) NOS	17 53 09.3	4.93	145.47	42	MS 7.0 (NOS) MB 6.0 (NOS)
(b) BMR Port Moresby	17 53 08.9	4.95	145.66	42	ML 7.1 (PMG)
(c) BMR Canberra	17 53 09.2	4.99	145.55	39	
(d) Modified (a)		4.95	145.69		
(e) Modified (c)		4.94	145.69		
Adopted	17 53 09.1	4.95	145.68	41	M 7.0

The NOS solution (a) was used as a basis for another determination using local stations within a radius of 7° from the epicentre. A plot of P residuals versus azimuth for these stations revealed that, by shifting the epicentre 25 km to the east, residuals were minimized. This is illustrated in Figure 4. The position of the epicentre thus derived is listed above as solution (d). A similar treatment of the BMR Canberra result gave the solution (e).

The two modified solutions and the BMR Port Moresby solution agree very closely and, in view of their coincidence with the region of greatest earthquake intensities, are considered to be the most reliable. This epicentral region is about 32 km north-northwest of Madang and about 12 km inland from the coast (Fig. 3). The assumed error in the NOS determination could partly or wholly result from a systematic network bias, which according to Lilwall & Underwood (1970) would cause NOS epicentres to be of the order of 12 km west of the true epicentre in the Madang region. (Their network bias for depth is negligible.)

Because the earthquake occurred centrally within the local network the network bias for HYPO epicentres should be minimal.

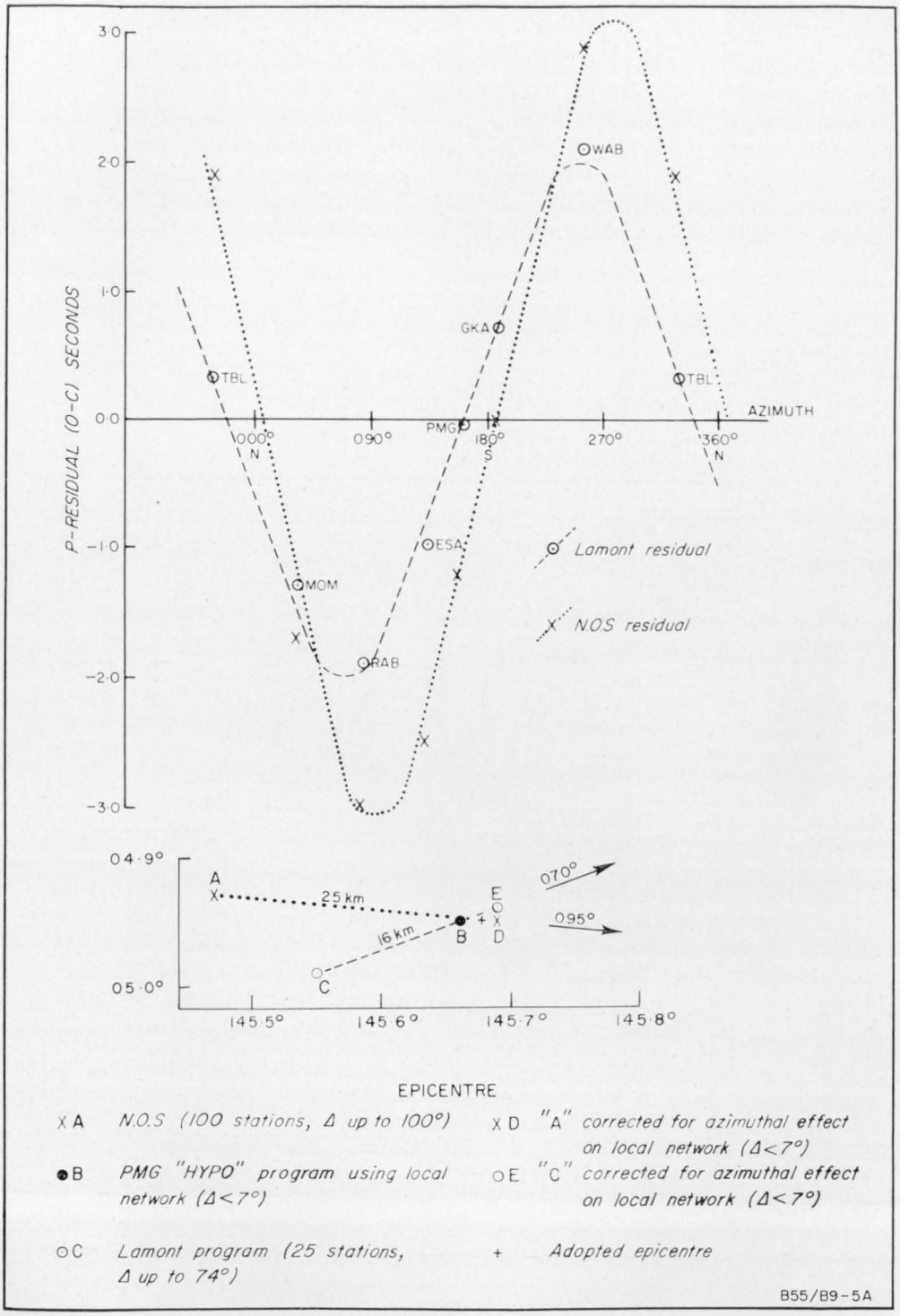

Fig. 4. P residual versus azimuth for the Madang earthquake, and corrected epicentres.

Foreshocks and aftershocks

Details of two foreshocks and the aftershocks recorded at Port Moresby and by NOS for the period 31 October 1970 to 30 April 1971 are included in Table 7 (at the back of the Report).

Parameters of about 200 earthquakes which occurred during the period 31 October to 27 November were calculated on an IBM 1130 computer using program HYPO. This program requires P times from local stations (within a radius of 10° from the epicentre) and at least one S-P interval in order to determine an epicentre, depth, and origin time for an event. From a series of tests it was found that by the use of S-P intervals from only the closest stations, i.e. less than about one degree from the epicentre, P residuals were minimized and the results agreed better with NOS results determined independently from P waves.

Accordingly the S-P interval at Madang (MAD) was largely relied on for origin times. S-P intervals from Tabele (TBL), on Manam Island, were used until 1000 UT on 1 November before recording commenced at Madang. The stations used for each determination of S-P are listed in Table 7, and details of the stations are listed in Table 1.

Systematic errors in hypocentre locations. Although the results of James et al. (1969) suggest relative accuracies of about 10 km and 20 km respectively for the epicentres and depths determined by the local network, systematic errors could also exist. This is demonstrated by the range of residuals (observed minus computed travel times) for the stations. The median values of P residuals with approximate epicentral distances and azimuths from the earthquakes for stations used most often were:

	PLN	*MAD*	*TBL*	*GKA*	*WAB*	*LAT*	*PMG*
RES (sec)	—1.7	—2.5	+3.1	—2.1	+0.9	+4.1	+1.8
DIST (°)	0.25	0.5	1.0	1.0	1.8	2.2	4.8
AZ (°)	—	160	320	180	250	145	150

Travel times of P waves to MAD were generally of the order of 10 seconds, so the residual of about 2.5 s (early arrival) is a large percentage of the travel time. It cannot be attributed to high local P-wave crustal velocity near Madang, because that would imply an unlikely velocity of 8 km/s instead of about 6 km/s. Systematic errors in origin time or hypocentre are the most likely cause of the large residuals at MAD and PLN.

NOS median residuals using earthquakes recorded by 10 or more stations were:

	MAD	*TBL*	*GKA*	*WAB*	*LAT*	*MOM*	*PMG*
RES	—0.5	+0.7	0.0	+1.0	+2.7	+0.3	+0.4

The NOS residuals are generally smaller than those for the local network determinations. However, LAT in both determinations has a large positive residual. Because arrivals of near-vertical teleseismic P waves at LAT are not markedly delayed by anomalous crustal or upper mantle structure beneath the station, it is considered that either a zone of unusually low velocity in the upper mantle or thick crust between the earthquake zone and LAT caused the large positive residuals from the Madang earthquake series. An analysis of LAT residuals versus azimuth for Papua New Guinea earthquakes could provide interesting information.

A least-squares mean position of accurately determined epicentres of aftershocks was determined from both HYPO and NOS data. Results were 4.86°S, 145.45°E for HYPO and 4.95°S, 145.48 for NOS; i.e. the local network position was about 10 km north of the NOS position. This fact along with negative residuals at MAD suggests that the HYPO epicentres may have a systematic error in position which places the epicentres too far north. On the other hand a systematic shift to the east would be required to eliminate the PLN residual (—1.7) and would result in better agreement with a mean position of seismic activity obtained from S-P data (discussed later).

Examination of the residuals did not lead to definite conclusions about their causes or the nature of systematic errors in the hypocentral data. However, the subject was introduced to ensure that the reader is aware of the possibilities of systematic errors, and to record the typical P residuals as they may be useful in further studies.

Foreshocks. Two foreshocks occurred about twelve hours before the principal earthquake (see Table 7). Both NOS and Port Moresby solutions indicated that the foreshock hypocentres were close to that of the main event. The largest of the foreshocks (MS 4.7) was felt at Madang with intensity MM4.

Aftershock pattern. Epicentres determined from the local network are plotted in Figures 5 and 6 and NOS epicentres in Figure 7.

The aftershock activity occurred in a zone trending east-northeast about 130 km long and 40 km wide, extending west-southwest from the vicinity of Karkar Island to the area around 5.2°S and 144.8°E. Focal depths mostly ranged from 10 to 60 km, and were concentrated around 30-40 km (Figs. 8 and 9).

The principal shock was near the southeastern margin of the aftershock region, and the area of aftershocks increased with lapse of time after the principal event. This is illustrated by comparing Figures 5 and 6; earthquakes to the end of 1 November (about one-fifth of the total, Fig. 5) occurred over a fairly restricted part of the total aftershock zone (Fig. 6).

The most westerly epicentre was that of the largest aftershock (12 November at 0607), and the NOS data (Fig. 7) show that events were concentrated in the southwestern part of the aftershock area as well as in the more central part. The occurrence of large aftershocks at the extremities of aftershock zones, and migrations of aftershock activity, are commonly observed in Japan and the Aleutian-Alaskan arc, according to Mogi (1968). Mogi also showed that two types of aftershock pattern occur: one is roughly circular (as observed in Japan); the other is elongated (as observed in the Aleutian-Alaskan arc). In both types the aftershock area extends with time as it did after the Madang event.

The elongated Madang aftershock pattern is similar to the Aleutian-Alaskan arc type. However, this may not be typical of the entire New Guinea region, because the patterns of aftershocks of a 1966 Solomon Island earthquake (Chouhan, Gaur & Rathor, 1970) and two major 1971 earthquakes in the north Solomon Sea (Everingham, 1973) appear to be more circular, similar to the Japanese type.

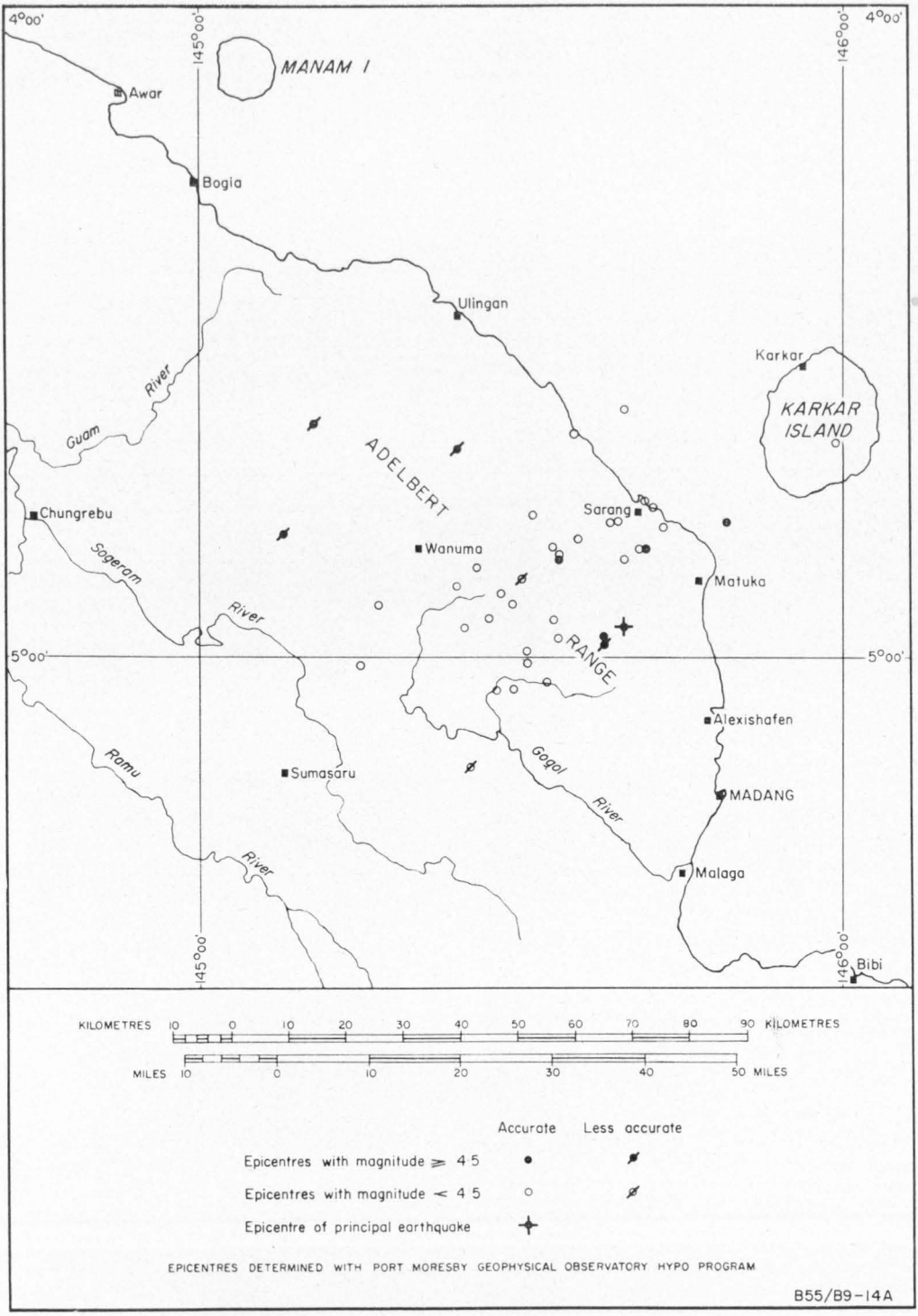

Fig. 5. HYPO epicentres of shocks for 31 October to 1 November 1970.

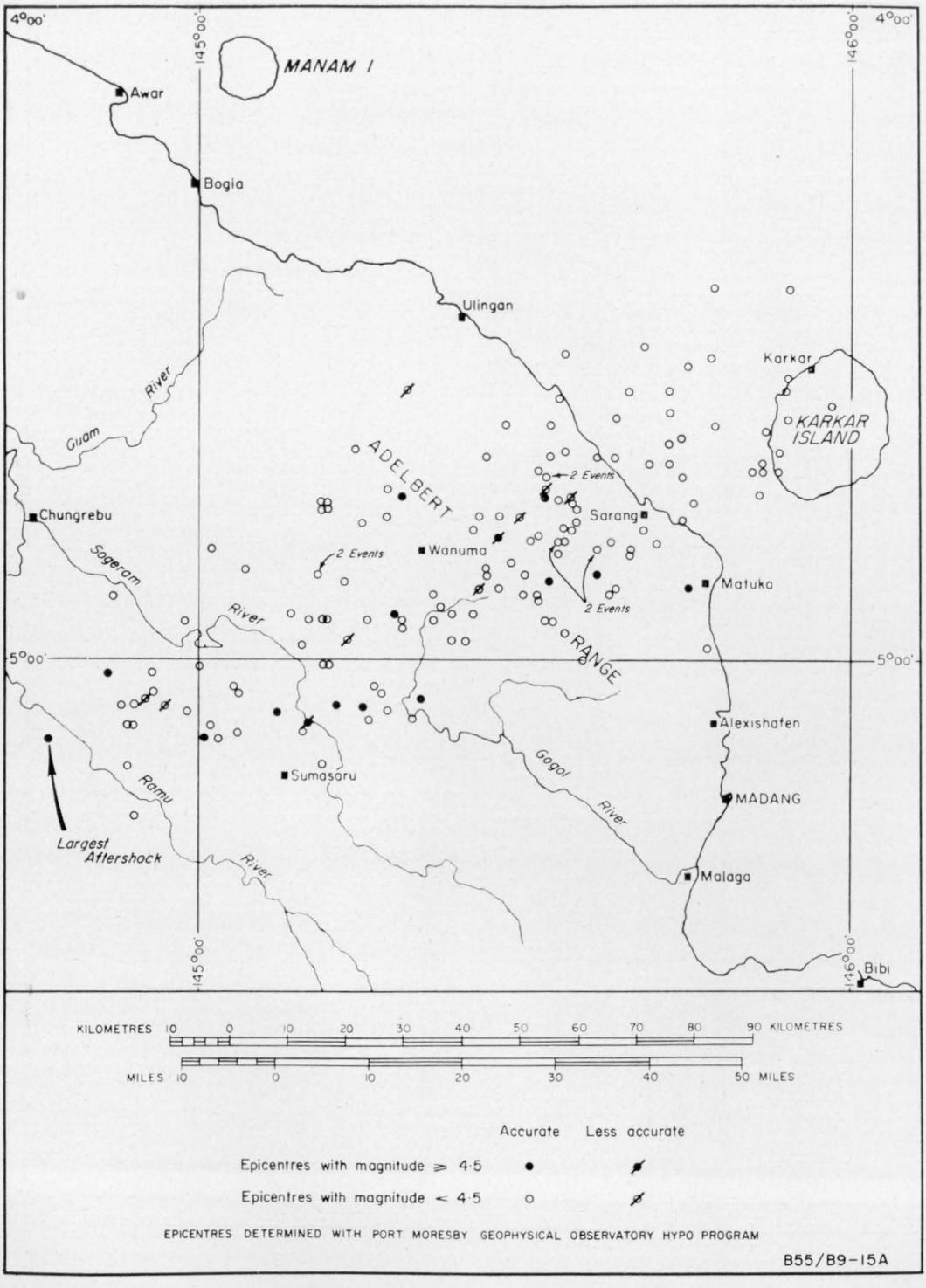

Fig. 6. HYPO epicentres of shocks for 2 November to 27 November 1970.

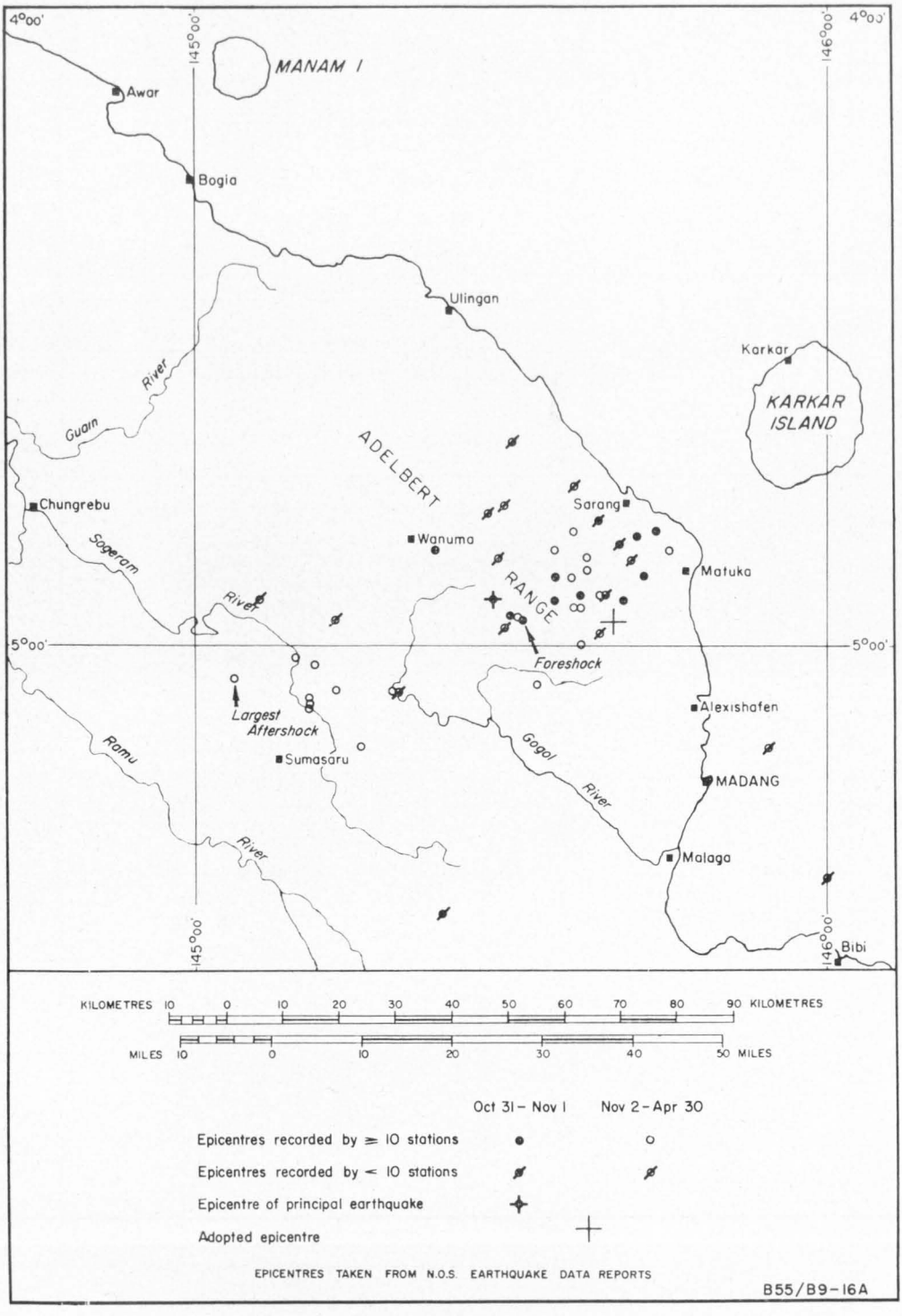

Fig. 7. NOS epicentres of shocks for 31 October 1970 to 30 April 1971.

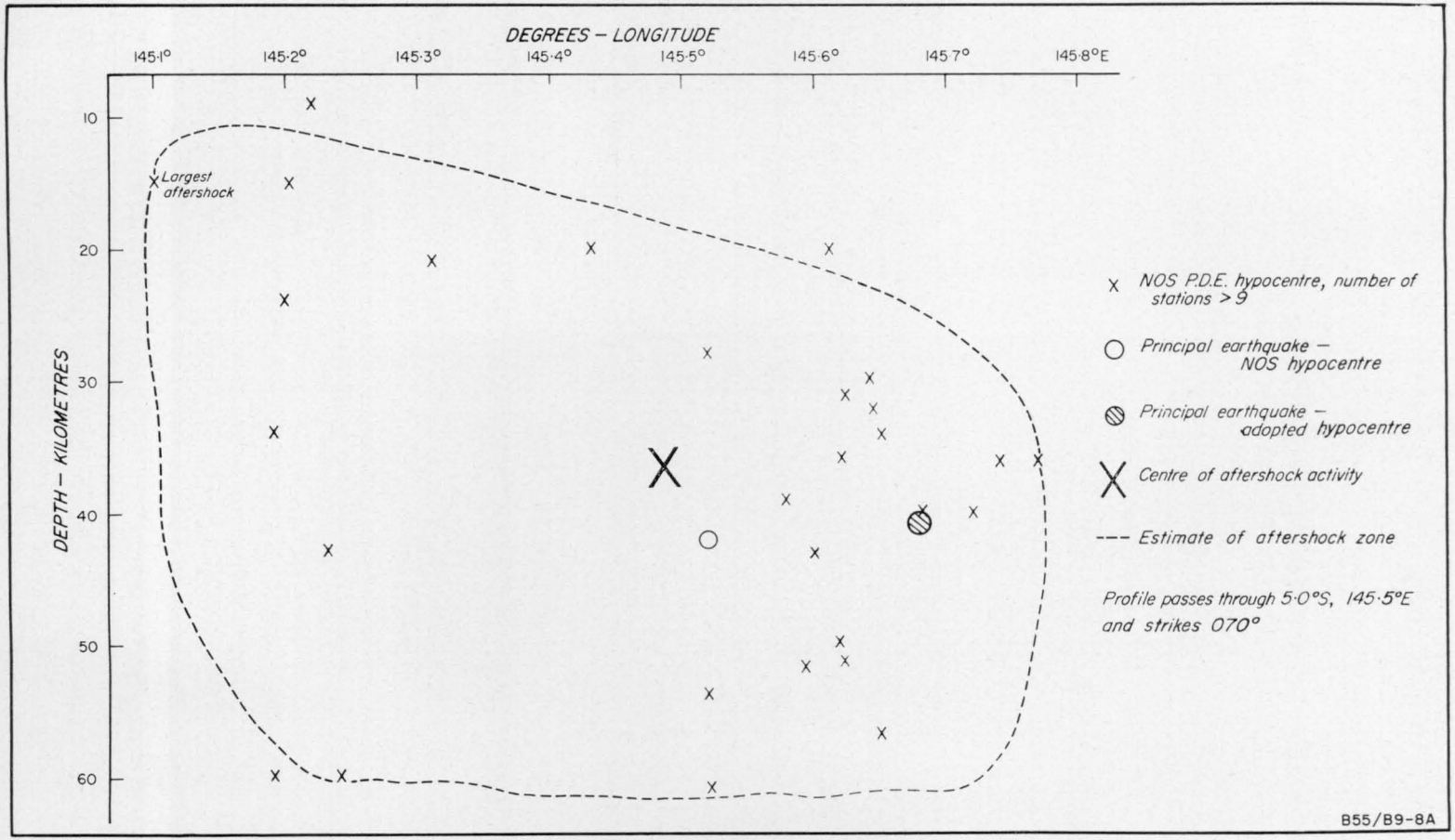

Fig. 8. Profile of aftershock zone in the direction 070°.

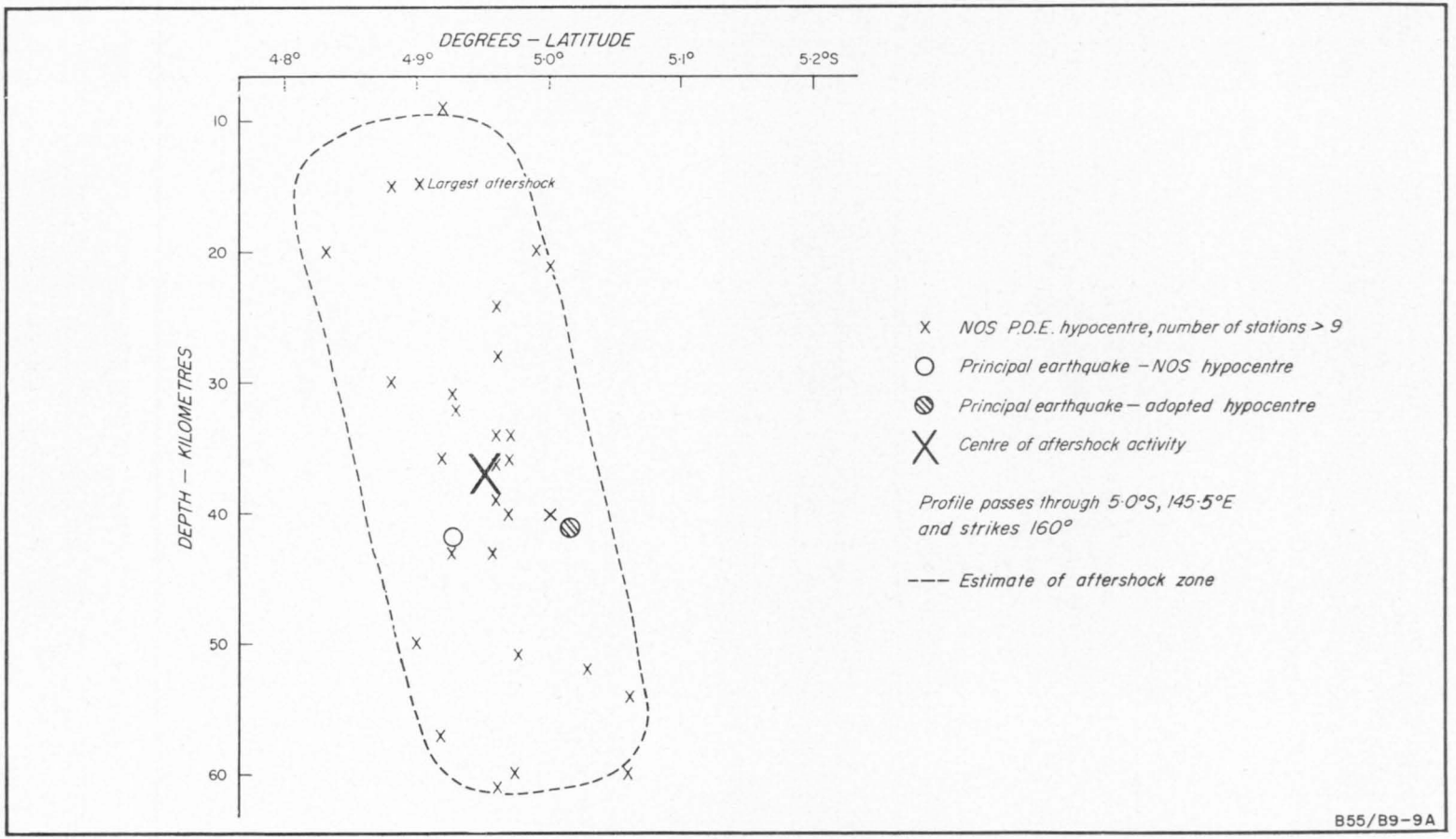

Fig. 9. Profile of aftershock zone in the direction 160°.

Profiles along and normal to the trend of the aftershock zone are shown in Figures 8 and 9. NOS data with 10 or more station readings were selected for plotting because their hypocentral depths were more reliable. Port Moresby hypocentral data, when plotted in the same manner, agreed generally with the NOS results, but because there were a greater number of events and more scatter in depths they indicated a larger zone of aftershock activity.

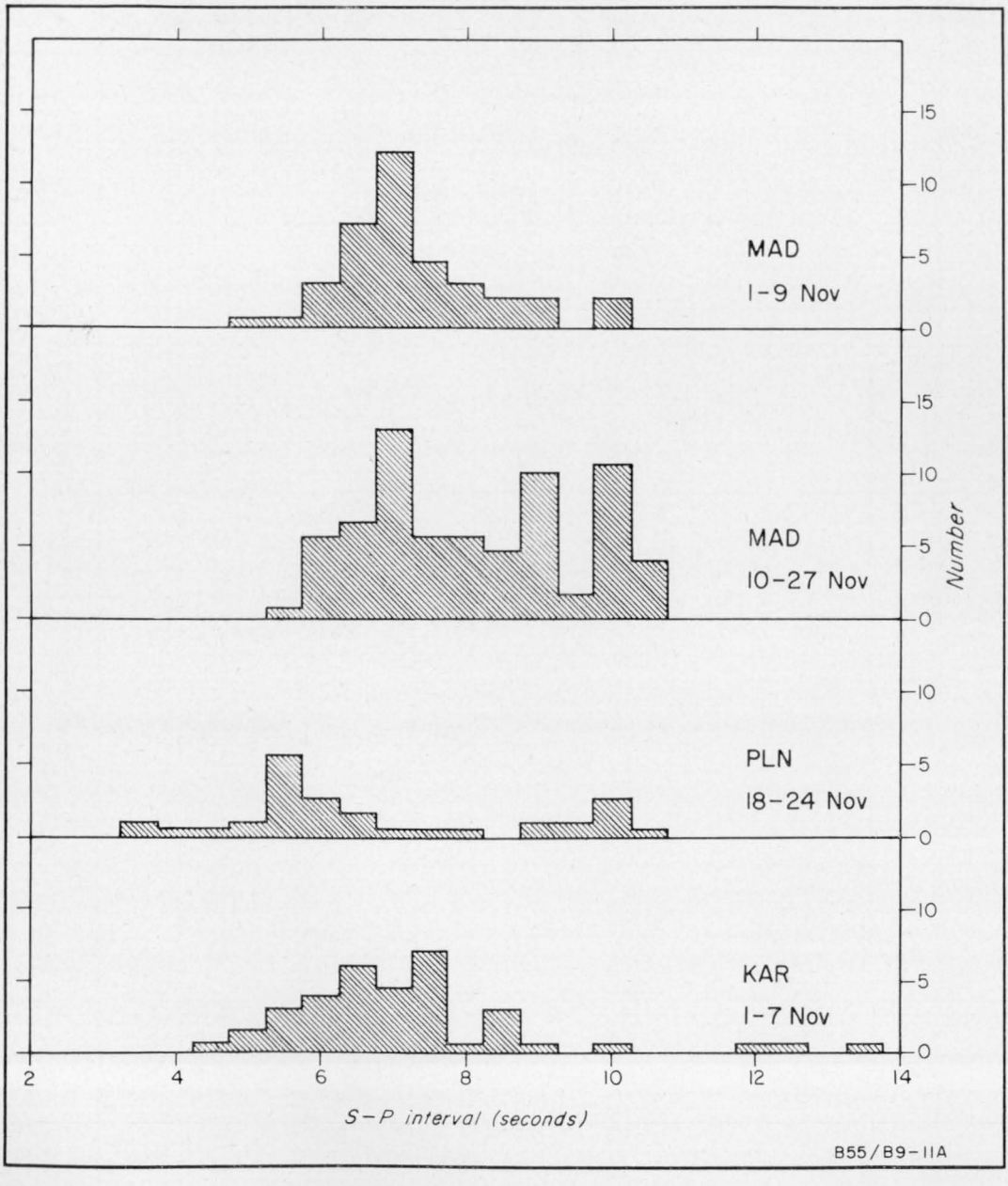

Fig. 10. Frequency of S-P intervals.

These profiles illustrate that the larger aftershocks were concentrated in a narrow, near-vertical zone about 20-30 km wide which extended horizontally about 80 km (in a direction 069°) and vertically downwards between depths of about 10 km and 60 km. The vertical extent of this aftershock zone averaged about 40 km and the volume was about 80 000 km^3. If the inaccuracy of hypocentral determination (± 10 km, say) could be removed, the zone might be much narrower and smaller in volume.

To find the position of the most concentrated aftershock activity, S-P intervals were plotted for several stations, the most commonly recorded intervals were related to distance from each station (via Jeffreys-Bullen tables for normal depth events), and a centre of main aftershock activity was then determined by the intersection of the arcs of S-P distances from the relevant stations.

The frequencies of S-P intervals for MAD, PLN, and KAR are plotted in Figure 10. The epicentre of most concentrated aftershock activity determined from S-P intervals was at latitude 4.85°S, longitude 145.53°E, i.e., 10 km north-northeast of the mean position indicated by NOS data and 10 km east of the mean position given by the HYPO data. The agreement with the NOS and HYPO results is good, but without knowing local standard travel times it is impossible to decide which method gives the most reliable result.

FAULT-PLANE SOLUTIONS

Attempts were made to obtain fault-plane solutions for 40 of the larger earthquakes in the series. Six were recorded well enough (Table 5) to give solutions, which are shown in Figure 11. Data from stations outside the local network were obtained from routine bulletins, from individual requests, and from seismograms. Station polarities were checked wherever possible by first motions recorded from a deep Fijian earthquake on 18 November 1970, which propagated a P-wave pulse of particularly large amplitude.

TABLE 5. PARAMETERS OF FAULT-PLANE SOLUTIONS

	NOS Epicentre		*Pole of Nodal Plane 1*		*Pole of Nodal Plane 2*		*T Axis*		*P Axis*	
Time	*Lat. °S*	*Long. °E*	*Az.°*	*Pl.°*	*Az.°*	*Pl.°*	*Az.°*	*Pl.°*	*Az.°*	*Pl.°*
Oct 31 1753	4.93	145.47	154	05	066	00	112	03	202	03
Nov 01 1107	4.82	145.73	146	00	058	10	103	07	012	07
Nov 02 1403	4.89	145.60	342	10	077	30	123	13	025	27
Nov 04 0404	5.09	145.18	173	00	263	30	302	22	213	22
Nov 12 0607	5.05	145.06	035	37	236	50	344	77	223	07
Dec 05 0952	4.94	145.61	155	16	048	50	118	45	003	20
						MEAN	306	07	023	04

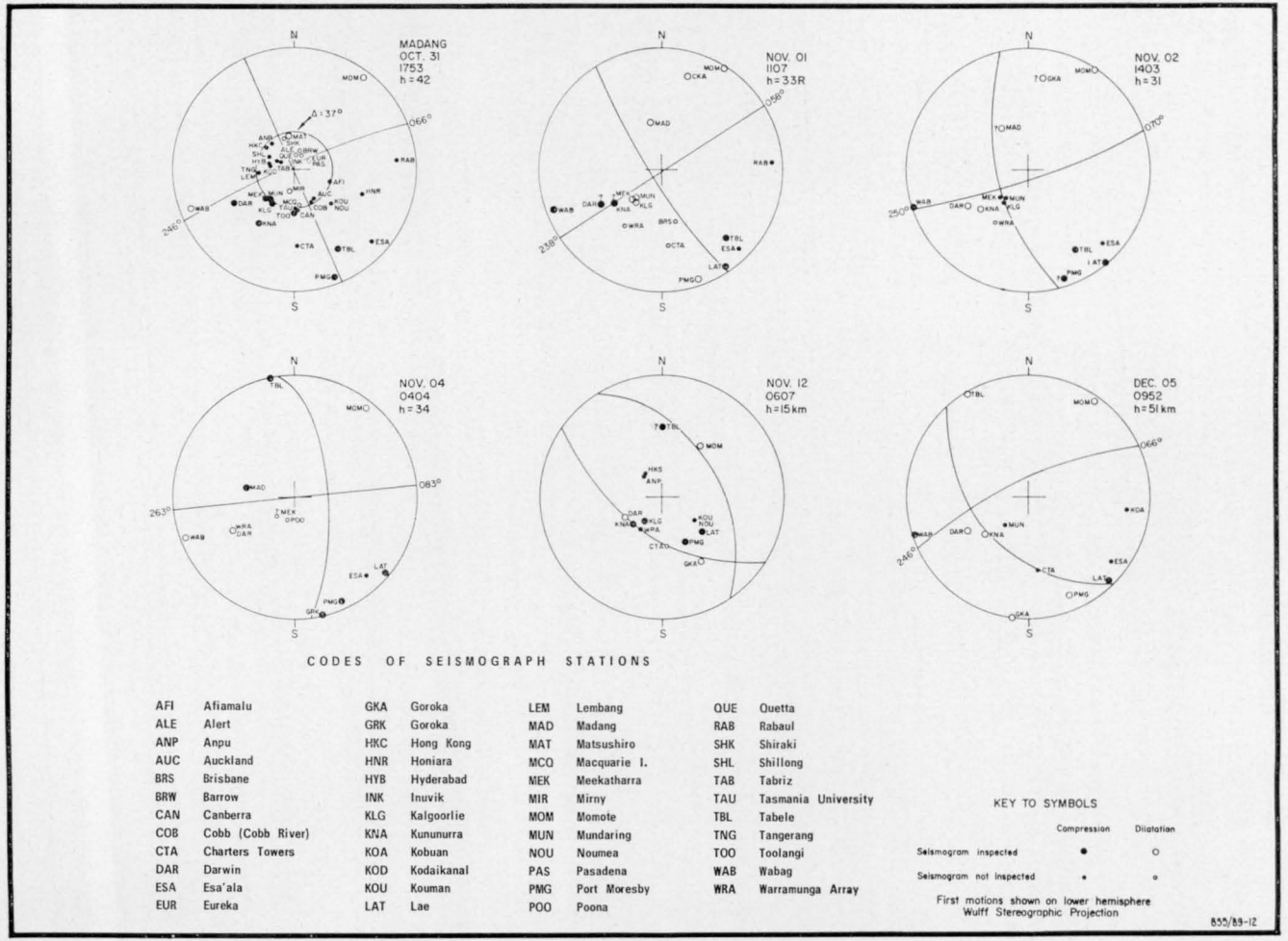

Fig. 11. Fault-plane solutions for the Madang earthquake series.

The fault-plane solution for the principal earthquake appeared to depend on the epicentral distance and station sensitivity. Data from stations at epicentral distances over about 37°, and some slightly closer low-gain stations which probably did not record the first motion, indicated sinistral transcurrent faulting striking 066° (or dextral transcurrent faulting striking 156°). Using closer stations and very high-gain stations on the Australian Shield, the solution indicated either near-vertical normal faulting striking 066° (northwest side up) or a near-horizontal overthrust from the east-southeast.

The pattern of aftershocks gives a clear indication of a near-vertical fault plane striking about 070°. Hence the first-motion data for the main event can be interpreted along the following lines. Roughly NNE-SSW compressive forces with a minor vertical component resulted in sinistral strike-slip faulting with a minor vertical movement, northwest side up, striking 070°. It is considered that the initial faulting was near-vertical dip-slip (northwest side up) and that subsequently (within a few seconds) transcurrent faulting occurred along the same plane. (All inspected seismograms showed a large increase in amplitude of P waves 4 to 5 seconds after the first arrival, which tends to confirm that the earthquake was a multiple event.)

With one exception, the solutions for aftershocks indicated continuing strike-slip movement along fault planes with roughly the same trend as for the principal event. The epicentre of each of these aftershocks was situated in the central part of the aftershock zone.

The solution for the largest aftershock (which happened on 12 November at the relatively shallow depth of 15 km, in the most westerly part of the aftershock region) differed from other solutions in that dip-slip faulting was indicated. Nevertheless the pressure axis was about the same as for the other events. Unfortunately, it was not possible to determine solutions for other shocks in this westerly area. The aftershock pattern suggests strike-slip faulting, but other modes are not precluded. Seismograms showed that at least two distinct types of earthquakes occurred in the Madang series and one of them propagated very emergent P phases which were unsuitable for fault-plane solutions. Hence the nature of the faulting associated with these events remains unknown.

The pattern of epicentres in Figure 1 appears to show zones of seismicity trending east-northeast: one includes the 1970 Madang earthquakes and passes to the north of Madang; the other, south of Madang, crosses the coast near Saidor. These trends in the pattern of seismicity suggest that active east-northeast faulting could be a feature of the region.

Because conclusive field evidence is scarce, the direction of movement that has taken place along the major northern New Guinea fault zones is speculative. Although the regional east-southeast strike of major faults is established (Dow, Smit, Bain & Ryburn, 1972), faults trending east-northeast, such as that deduced from the Madang earthquake, have been mapped but they are uncommon. For example, the Papua New Guinea Geological Survey's unpublished regional maps of the area around Madang show this type of movement, viz. sinistral strike-slip and an east-northeast trend, at only one fault. If the regional stress is NNE-SSW compression the east-northeast faulting should be sinistral.

A regional NNE-SSW compressive stress, as suggested by the Madang earthquake data, was previously inferred by Denham (1969). Because of the pattern of seismicity in Papua New Guinea he considered that the Indian-Australian Plate should be moving north-northeast relative to the Pacific Plate and not about 075° as suggested by Le Pichon (1968), and surmised that, because the Pacific Plate to the north of New Guinea was in the shadow zone of the Tonga Trench, it would be immobile.

Ripper's (in press) fault-plane solutions for the northern New Guinea region suggest north-northeast compression in the Madang-Lae area where the South Bismarck Sea subplate contacts the Indian-Australian Plate. However, this is a local effect (Krause, 1972) at the junction of two plates, and generally the New Guinea fault-plane solutions are consistent with Le Pichon's direction.

MAGNITUDE/FREQUENCY RESULTS

Magnitude/frequency relations for the Madang aftershock series are presented for comparison with similar relations found for global and regional areas. Magnitude nomenclature used at the Port Moresby Observatory (PMG) is:

ML (PMG) = local magnitude (Richter, 1958) determined from the mean horizontal trace deflection on the PMG standard Wood-Anderson seismograms.

MS (PMG) = magnitude determined from maximum amplitude of surface-wave train measured on the Worldwide Standard Seismograph long-period vertical record (≈MS(NOS)).

MB (PMG) = magnitude determined from maximum amplitude of P-wave train on the Worldwide Standard Seismograph short-period vertical record (≈MB(NOS)).

MB (NOS) = NOS body-wave magnitude using only data for epicentral distances over 25°.

MS (NOS) = NOS surface-wave magnitude ($= \log A/T + 1.66 \log A + 3.3$)

M = unified surface-wave magnitude: the mean of MS and MB and ML converted to MS equivalent; it is also used as a general term for magnitude.

The relations between the various magnitude scales, their derivation, and methods used to determine the magnitudes are given separately (Everingham, in prep. b). It is emphasized that magnitudes were measured by reference to PMG seismograms; the distance between PMG and the aftershocks was assumed to be constant (4.8°).

The generally accepted magnitude/frequency relation is:

$$\text{Log } N = A - bM$$

where

N is number of events with magnitudes equal to or greater than M occurring during a given interval

b relates number of events with magnitude M to the number of events with magnitude $M + 1$

A indicates the degree of seismic activity.

The magnitude/frequency data extracted from Table 7 (to 30 November) are summarized in Table 6. Several aftershocks that occurred within a few hours after the principal event, when seismograms were sometimes indecipherable, are not listed in Table 7; however, it was assumed that the number of missing aftershocks of a given magnitude was inversely proportional to that magnitude so that the magnitude/frequency plot would not be greatly affected.

TABLE 6. MAGNITUDE/FREQUENCY DATA FOR AFTERSHOCKS

	ML (PMG)	*MS (PMG)*	*MB (PMG)*
Mag.	*N*	*N*	*N*
3.1		83	196
3.2		82	196
3.3	NOTE: Italic figures used in	81	*196*
3.4	log $N = A—bM$ analysis	*81*	*163*
3.5		*70*	*114*
3.6		*56*	*104*
3.7		*45*	*100*
3.8		*38*	*88*
3.9		*33*	*75*
4.0		*24*	*63*
4.1		*22*	*54*
4.2		*18*	*44*
4.3		*17*	*39*
4.4	47	*17*	*37*
4.5	46	*15*	*27*
4.6	44	*13*	*23*
4.7	*42*	*8*	*19*
4.8	*33*	*8*	*16*
4.9	*22*	*8*	*14*
5.0	*14*	*8*	*12*
5.1	*8*	*8*	*8*
5.2	*7*	*8*	*7*
5.3	*6*	*5*	*6*
5.4	6	5	4
5.5	4	2	4
5.6	4	2	2
5.7	2	2	1
5.8	2	2	1
5.9	2	2	1
6.0	1	2	0
6.1	1	2	
6.2	1	2	
6.3	1		
6.4	1		
6.5	0		

The values of A and b found for the Madang aftershocks using least-squares analysis are tabulated below along with other results (marked by asterisks) to facilitate comparisons of the b-factors. In the determination of A and b the lower magnitude cut-off point (below which magnitudes are too small for data to be recorded reliably) was determined by inspection from graphs of N versus magnitude: the upper magnitude cut-off point was chosen arbitrarily to exclude magnitudes where N was less than 5.

Mag. Type	*Mag. Range*	*A*	*b*
MS(PMG)	3.4–5.4	3.99 ± 0.13	0.59 ± 0.03
*MS(NOS)	5.4–6.4	6.5	0.73
***MS(NOS)	5.3–6.8	4.5 to 7.5	0.5 to 1.0
MB(PMG)	3.3–5.3	4.71 ± 0.07	0.73 ± 0.01
*MB(NOS)	5.5–6.0	9.35	1.25
**MB(NOS)	(5.0–6.0?)	8.00	1.16
ML(PMG)	4.7–5.4	7.94 ± 0.72	1.35 ± 0.14
***ML(PMG)	5.6–6.1	7.24	0.87

Results clearly show that, for each magnitude scale, there appears to be no general agreement between the *b*-values for the Madang aftershock sequence, regional seismicity, and global seismicity; i.e. for the *b*-values determined from the Madang sequence, the ML value is higher than the regional value, the MS value is slightly lower than the global value, and the MB value is much lower than both the regional and global values. From studies of seismicity in other regions, Wyss (1973) concluded that low *b*-values are associated with high stress in the source region; presumably higher *b*-values are associated with low stress. As the main shock of an earthquake should decrease the local tectonic stress to a considerable degree, aftershocks would be expected to have higher *b*-values than regional (and possibly global) seismicity, but the MS and MB values for the Madang aftershock sequence are anomalous, for their *b*-values are lower than those for global (and, for MB, regional) seismicity.

It is interesting to compare the Madang magnitude/frequency data with those of the aftershock sequence for the Solomon Islands earthquake of 15 June 1966, which had about the same magnitude, viz. MB (NOS) = 6.2, but a dip-slip fault-plane solution (Johnson & Molnar, 1972). For aftershocks of this event Chouhan et al. (1970) calculated that:

$$\text{Log } N = 5.07 - 0.76 \text{ MB(NOS)}$$

These *A* and *b* values are remarkably close to the Madang body-wave values, 4.71 and 0.73 respectively.

The magnitude/frequency relations show that there were slightly over one-and-a-half times the number of aftershocks of a given magnitude in the Solomon Island series than in the Madang series.

CONCLUSIONS

(a) The Madang earthquake details are:
Origin time—1753 09.1 UT 31 October 1970
Focal depth—41 km
Epicentre—4.95°S, 145.68°E
Magnitude—M 7.0

* Graphical solution (by eye) using 1969 and 1970 global earthquakes for which both MB(NOS) and MS(NOS) were determined.

** Denham (1969) using 1958-1966 Papua New Guinea/Solomon Islands events.

*** Graphical solution for regional value (by eye) using 1969, 1970, and 1971 Papua New Guinea/Solomon Islands events.

(b) The maximum intensity was at least MM8, and damaging intensities of MM7 and greater were experienced over an area of roughly 10 000 km^2. Damage was estimated at $1.7 million, and 15 lives were lost. Well designed buildings were undamaged at Madang. Intense landsliding occurred within the MM8 isoseismal.

(c) A small tsunami was generated by submarine slides.

(d) Locations and magnitudes of about 200 aftershocks were determined. For aftershocks, log $N = 4.71 - 0.73$ MB(PMG). The b-factor, 0.73, is markedly lower than the value 1.2 found for regional and global seismicity.

(e) The aftershock area, which expanded with lapse of time after the principal earthquake, was elongated in the direction 069° and extended about 130 km. The active volume was about 80 000 km^3. Larger events were in the depth range 10-60 km and concentrated around 40 km.

(f) P-wave travel-times to LAT, about 2.4° from the centre of the aftershock zone, were anomalous, being about 3 seconds longer than expected.

(g) Fault-plane solutions for five aftershocks, and aftershock pattern, suggested that the Madang earthquake was caused by sinistral strike-slip faulting in the direction 069°; the faulting would result from regional NNE-SSW compression. The only event that gave a dip-slip fault-plane solution was the largest aftershock (12 November); however, this solution was also consistent with NNE-SSW compression.

(h) Future earthquakes should be studied along the same lines as reported here, particularly the aftershock distribution in space, time, and magnitude, so that enough data can be accumulated to permit more definite conclusions on the nature and causes of features of earthquake series.

ACKNOWLEDGEMENTS

The following are gratefully acknowledged for the valuable assistance they rendered during the investigation of the Madang earthquake and aftershocks: the Department of District Administration's staff at Madang for air and ground transport and for information on the earthquake; the Civil Defence Department at Port Moresby for arranging the air charter to Madang on the day of the earthquake; the Rabaul Central Observatory for supplying records and data; and the Overseas Telecommunications Commission for supplying information on the SEACOM cable damage.

TABLE 7. MADANG EARTHQUAKE SERIES — PMG AND (*) NOS DATA

Date 1970	Origin Time UT	Epicentre Lat. °S	Epicentre Long. °E	Depth km	Magnitude ML	Magnitude MS	Magnitude MB	S-P Stn	No. Stns	EDR No.
Oct.										
31	05 44 35.4	4.99	145.51	33R	4.7	3.6	4.2	TBL		
31	06 19 41.4	(4.98)	(145.63)	(33R)	5.0	4.7	4.9	TBL		
*	06 19 40.7	4.96	145.52	37	—	—	—	*	13	76
31	17 53 08.9	4.95	145.66	42	7.1	—	—	TBL, PMG, RAB		
*	17 53 09.3	4.93	145.47	42	—	7.0	6.0	*	100	74
31	18 43 06.3	(4.81)	(145.13)	(214)	4.8	—	—	PMG		
*	18 43 09.7	4.89	145.71	40	—	—	5.0	*	11	74
31	— — —	—	—	—	4.9	—	—			
*	18 47 43.8	4.89	145.57	43	—	—	4.6	*	17	74
31	— — —	—	—	—	4.9	—	5.0			
*	19 07 00.1	4.83	145.70	36	—	—	4.9	*	14	74
Nov.										
01	00 01 26.0	(4.64)	(145.18)	(169)	4.9	4.6	4.9	PMG		
*	00 01 31.2	4.92	145.61	36	—	—	—	*	13	73
01	00 30 56.4	4.97	145.56	33R	4.7	3.6	3.9	TBL		
01	01 24 49.3	(4.68)	(145.40)	(132)	4.5	3.9	4.5	WAB, PMG		
*	01 24 52.4	4.80	145.64	56	—	—	—	*	8	76
01	— — —	—	—	—	4.7	4.6	4.7			
*	01 33 04.3	4.85	145.38	20	—	—	5.1	*	16	73
01	02 16 20.2	4.92	145.49	33R	—	3.9	4.2	TBL		
01	02 44 29.1	5.05	145.46	33R	—	3.2	3.9	TBL		
01	02 53 18.7	4.90	145.47	84	—	3.7	4.1	TBL		
01	03 45 52.9	(5.17)	(145.42)	(33R)	—	3.6	4.0	TBL		
01	05 00 20.6	5.05	145.49	33R	—	—	3.4	TBL		
01	05 16 15.6	5.04	145.54	33R	—	—	4.0	TBL		
01	05 27 48.0	4.94	145.55	33R	4.7	3.9	4.0	TBL		
*	05 27 46.4	4.95	145.50	61	—	—	—	*	10	74
01	05 42 42.1	4.97	145.63	33R	4.6	3.7	4.5	TBL		
*	05 42 44.9	5.42	145.39	54	—	—	—	*	7	76
01	08 01 57.6	5.01	145.51	33R	—	3.5	4.1	TBL		
01	08 45 37.9	4.94	145.45	42	—	—	3.7	TBL		
01	09 03 55.7	4.92	145.28	83	—	—	3.7	TBL		
01	09 31 44.5	(4.88)	(145.50)	(35)	—	—	3.1	TBL		

TABLE 7. MADANG EARTHQUAKE SERIES — PMG AND (*) NOS DATA (*cont.*)

Date 1970	*Origin Time* UT	*Epicentre* Lat. °S	Long. °E	*Depth* km	*Magnitude* ML	MS	MB	*S-P* Stn	*No.* Stns	*EDR* No.
01	10 08 02.5	4.83	145.55	51	—	3.6	3.9	MAD		
01	10 41 36.3	4.77	145.70	37	—	3.7	4.0	MAD		
01	11 07 41.5	4.79	145.82	33R	5.9	6.1	5.6	MAD		
*	11 07 40.6	4.82	145.73	33R	—	5.1	5.5	*	68	74
01	12 43 57.3	4.95	145.41	76	—	3.5	4.2	MAD		
01	13 07 30.9	4.79	145.65	53	—	—	3.1	MAD		
01	14 03 36.9	5.01	145.25	48	—	3.7	4.1	MAD		
01	14 49 31.7	4.85	145.66	45	—	3.8	4.3	MAD		
01	14 56 34.2	4.78	145.52	53	—	3.4	3.9	MAD		
01	15 29 57.9	4.67	145.99	33R	—	—	3.8	MAD		
01	15 35 46.8	4.85	145.56	73	5.0	4.6	5.1	MAD		
*	15 35 48.8	4.93	145.68	40	—	—	4.9	*	16	75
01	15 46 52.4	4.86	145.43	75	4.8	4.5	4.4	MAD		
*	15 46 54.7	4.93	145.57	39	—	—	4.4	*	12	76
01	16 03 42.2	4.83	145.68	33R	—	3.4	3.9	MAD		
01	16 53 37.1	4.80	145.72	40	—	—	3.5	MAD		
01	18 28 18.7	4.66	145.58	48	—	—	3.4	MAD		
01	19 27 11.4	4.76	145.69	52	5.0	3.5	4.1	MAD		
01	19 48 52.9	4.79	145.64	46	—	—	3.4	MAD		
01	20 55 07.9	4.82	145.59	44	—	3.4	3.7	MAD		
01	21 13 14.7	4.62	145.66	60	—	—	3.4	MAD		
01	22 15 08.8	4.83	145.69	50	4.7	3.7	4.5	MAD		
*	22 15 09.1	4.84	145.67	37	—	—	—	*	7	76
01	22 20 49.3	4.89	145.40	39	—	—	3.1	MAD		
01	23 04 38.1	4.84	145.56	39	—	—	3.4	MAD		
02	02 48 55.5	4.81	145.52	46	—	—	3.7	MAD		
02	03 16 05.9	4.72	145.53	64	—	—	3.7	MAD		
02	05 05 34.4	4.84	145.55	51	—	3.6	4.2	MAD		
02	05 42 53.5	4.89	145.64	33R	—	—	3.8	MAD, KAR		
02	07 05 25.1	4.90	145.50	35	4.7	3.5	4.0	MAD, KAR		
*	07 05 24.0	4.79	145.46	33R	—	—	—	*	6	76
02	07 25 46.8	4.67	145.72	71	—	—	3.5	MAD		
02	09 09 03.4	4.90	145.63	56	4.7	—	4.1	MAD		
*	09 09 00.7	4.68	145.50	21	—	—	—	*	7	76

TABLE 7. MADANG EARTHQUAKE SERIES — PMG AND (*) NOS DATA (*cont.*)

Date 1970	*Origin Time* UT	*Epicentre* Lat. °S	Long. °E	*Depth* km	*Magnitude* ML	MS	MB	*S-P* Stn	*No.* Stns	*EDR* No.
02	11 08 49.9	4.80	145.42	65	—	—	3.4	MAD		
02	13 36 34.4	4.87	145.44	66	—	3.8	4.2	MAD		
*	13 36 35.9	4.86	145.69	38	—	—	4.9	*	8	73
02	14 01 01.3	4.82	145.55	47	—	—	3.7	MAD		
02	14 03 13.4	4.88	145.54	54	5.6	5.1	5.5	MAD		
*	14 03 13.4	4.89	145.60	31	—	5.6	5.0	*	28	73
02	15 30 37.4	4.77	145.58	55	—	—	3.8	MAD		
02	20 45 54.2	4.63	145.64	33R	—	—	3.8	MAD		
02	21 32 22.3	4.69	145.64	76	—	—	3.7	MAD		
02	21 46 40.0	4.75	145.53	52	5.0	4.1	4.5	MAD		
*	21 46 42.2	4.86	145.48	54	—	—	—	*	7	77
02	23 00 30.9	4.93	145.42	44	—	3.4	4.0	MAD		
03	00 00 47.9	4.92	145.37	50	—	—	3.4	MAD		
03	00 21 42.9	4.93	145.30	35	4.9	4.0	4.6	MAD		
*	00 21 43.3	4.97	145.49	41	—	—	—	*	9	75
03	03 33 19.0	4.97	145.41	33R	—	—	3.4	MAD		
03	04 08 30.8	4.95	145.31	46	4.8	3.9	4.4	MAD		
*	04 08 31.6	4.95	145.51	28	—	—	—	*	10	75
03	06 14 23.0	4.69	145.54	62	—	—	3.4	MAD		
03	09 12 08.7	4.90	145.52	49	—	3.5	4.0	MAD		
03	09 51 31.1	4.76	145.57	66	—	—	3.4	MAD		
03	10 19 40.5	4.82	145.56	45	—	—	3.1	MAD		
03	11 55 45.2	5.05	145.06	33R	—	3.4	3.9	MAD		
03	12 03 47.0	4.94	145.20	35	—	3.6	4.1	MAD		
03	12 51 10.8	5.07	145.25	33R	5.0	5.4	5.3	MAD		
*	12 51 09.5	5.08	145.18	24	—	—	5.2	*	23	75
03	16 27 28.4	4.83	145.02	61	—	3.5	3.8	MAD		
03	17 18 40.3	4.78	145.29	64	—	3.8	4.4	MAD		
03	20 00 56.2	4.94	145.36	46	—	3.4	4.0	MAD		
03	22 16 54.7	4.93	145.14	49	—	3.5	4.1	MAD		
04	00 01 52.6	4.83	145.61	42	—	—	3.6	MAD		
04	02 32 11.8	4.79	145.58	48	—	—	3.4	MAD		
04	03 05 00.7	5.07	145.21	33R	4.9	5.2	4.6	MAD		
*	03 04 57.2	4.96	145.22	10	—	—	4.7	*	9	79

TABLE 7. MADANG EARTHQUAKE SERIES — PMG AND (*) NOS DATA (*cont.*)

Date 1970	*Origin Time* UT	*Epicentre* Lat. °S	Long. °E	*Depth* km	*Magnitude* ML	MS	MB	*S-P* Stn	*No.* Stns	*EDR* No.
04	03 28 58.0	4.69	145.44	44	—	3.6	3.9	MAD		
04	04 03 56.5	5.06	145.34	33R	5.1	5.4	5.3	MAD		
*	04 03 54.1	5.09	145.18	34	—	—	5.1	*	24	75
04	08 39 19.5	4.80	145.57	58	—	—	3.4	MAD		
04	15 24 26.2	4.82	145.55	54	5.0	4.1	4.7	MAD		
*	15 24 26.4	4.85	145.57	50	—	—	—	*	10	75
04	15 49 16.5	5.16	144.89	33R	—	—	3.1	MAD		
04	17 15 18.8	5.07	144.90	41	—	3.5	3.7	MAD		
04	19 04 27.7	(4.75)	(145.57)	(80)	—	3.4	3.4	MAD		
04	19 47 20.4	4.97	145.39	58	—	—	3.4	MAD		
04	21 23 58.7	5.12	145.01	40	4.8	4.6	4.8	MAD		
*	21 23 58.8	5.02	145.16	15	—	—	4.6	*	13	75
04	22 18 17.5	4.91	145.52	35	—	—	3.4	MAD		
05	02 47 26.7	5.10	145.02	59	—	—	3.9	MAD		
05	03 35 10.6	4.83	145.61	54	—	—	3.4	MAD		
05	04 49 54.2	5.10	144.89	53	—	—	3.4	MAD		
05	06 26 11.3	4.96	145.56	23	—	—	3.1	MAD, SUM		
05	06 54 10.7	5.09	145.33	33R	—	—	3.5	MAD		
05	11 06 46.1	4.59	145.66	45	—	—	3.1	MAD		
05	22 08 19.3	4.68	145.89	33R	—	3.5	3.7	MAD		
06	07 19 38.3	4.75	145.55	66	—	—	3.4	MAD		
06	12 55 15.1	4.60	145.55	67	—	—	3.5	MAD		
06	16 08 25.5	4.87	145.50	47	—	—	3.4	MAD		
06	19 52 05.4	(5.07)	(144.95)	(19)	—	—	3.4	MAD		
06	21 22 35.1	4.64	145.47	68	—	—	3.6	MAD		
06	21 30 31.0	4.53	145.56	78	—	—	3.1	MAD		
06	22 30 36.4	4.85	145.48	72	—	—	3.4	MAD		
06	23 44 02.0	4.90	144.87	84	—	3.4	3.8	TBL		
07	22 25 27.4	4.94	145.53	70	—	3.5	4.4	MAD		
*	22 25 29.5	4.98	145.64	64	—	—	—	*	6	78
08	05 03 31.9	4.89	145.46	56	—	—	3.4	MAD		
08	08 56 01.1	4.64	145.54	52	—	—	3.4	MAD		
08	12 47 36.1	4.75	145.31	86	—	3.8	4.7	MAD		
*	12 47 39.8	4.75	145.60	43	—	—	—	*	9	76

TABLE 7. MADANG EARTHQUAKE SERIES — PMG AND (*) NOS DATA (*cont.*)

Date 1970	*Origin Time* UT	*Epicentre* Lat. °S	Long. °E	*Depth* km	*Magnitude* ML	MS	MB	*S-P* Stn	*No.* Stns	*EDR* No.
08	14 40 21.0	4.72	145.53	76	—	—	3.5	MAD		
08	15 15 06.6	4.68	145.56	39	—	—	4.4	MAD		
08	17 43 52.9	5.88	146.03	66	—	—	3.4	MAD		
08	19 45 37.1	4.77	145.20	70	—	—	3.4	MAD		
08	20 32 26.6	(5.06)	(144.92)	(13)	—	3.9	4.4	MAD		
09	02 51 11.5	4.82	145.70	35	—	—	3.7	MAD		
09	05 27 40.3	4.70	145.69	47	—	—	3.4	MAD		
09	14 00 13.6	4.83	145.66	39	—	—	3.4	MAD		
09	18 27 39.0	(4.97)	(145.23)	(110)	—	4.0	4.4	MAD		
09	22 11 59.7	4.64	145.79	44	—	—	3.4	MAD		
10	02 44 12.5	4.71	145.85	35	—	—	3.4	MAD		
10	08 51 09.9	(4.74)	(145.53)	(99)	4.7	4.2	4.4	MAD		
*	08 51 12.9	4.94	145.60	20	—	—	—	*	10	77
10	17 22 45.3	4.57	145.90	33R	—	—	3.4	MAD		
10	18 12 59.9	(4.89)	(145.43)	(89)	—	3.4	3.8	MAD		
11	01 14 47.8	4.72	145.74	51	—	—	3.1	MAD		
11	05 08 17.9	5.01	145.19	33R	4.5	3.7	4.1	MAD		
11	06 25 58.5	4.82	145.51	57	—	—	3.1	MAD		
12	02 27 46.2	4.89	145.75	35	5.0	4.1	4.9	WAB, LAT, PMG		
*	02 27 45.0	4.82	145.60	30	—	—	4.9	*	11	75
12	06 07 11.2	5.12	144.77	86	6.4	—	—	MAD		
*	06 07 12.4	5.05	145.06	15	—	6.5	5.9	*	58	75
12	06 41 47.5	5.02	144.86	33R	4.8	—	4.5	MAD		
*	06 41 47.3	4.93	145.10	6	—	—	—	*	9	75
12	07 21 28.7	(5.11)	(144.58)	(105)	4.8	—	4.7	MAD		
*	07 21 33.3	5.03	145.19	9	—	—	4.3	*	11	78
12	08 19 46.7	5.24	144.90	33R	—	—	4.2	MAD		
*	08 19 48.4	5.07	145.32	37	—	—	—	*	6	78
12	09 01 19.0	5.07	144.88	56	—	—	3.5	MAD		
12	09 39 41.5	5.06	144.90	56	—	—	—	MAD		
12	12 42 13.3	5.01	145.00	65	—	3.5	3.7	MAD		
12	14 30 50.1	4.76	145.20	95	—	—	3.1	MAD		
12	16 25 48.1	4.78	145.46	90	4.7	3.5	4.1	MAD		
*	16 25 49.3	4.78	145.49	43	—	—	—	*	7	76

TABLE 7. MADANG EARTHQUAKE SERIES — PMG AND (*) NOS DATA (*cont.*)

Date 1970	*Origin Time* UT	*Epicentre* Lat. °S	Long. °E	*Depth* km	*Magnitude* ML	MS	MB	*S-P* Stn	*No.* Stns	*EDR* No.
12	18 19 36.9	5.16	145.19	34	—	3.8	3.8	MAD		
12	21 35 26.5	5.05	144.93	55	—	—	3.4	MAD		
12	23 35 37.8	4.71	145.52	57	—	—	3.1	MAD		
13	00 41 06.4	5.12	145.03	45	—	—	3.4	MAD		
13	01 03 40.0	5.08	145.12	72	5.4	5.4	4.8	MAD		
*	01 03 40.6	5.07	145.31	21	—	—	4.8	*	15	75
13	01 21 26.6	5.05	145.28	85	—	—	3.4	MAD		
13	01 25 32.4	5.02	144.93	69	—	—	3.4	MAD		
13	01 34 51.8	4.87	145.18	99	—	3.5	3.9	MAD		
13	07 48 22.4	5.11	145.06	68	—	—	3.4	MAD		
13	08 11 46.0	4.88	145.22	76	—	—	3.1	MAD		
13	11 31 59.7	4.77	145.19	78	—	—	3.4	MAD		
13	12 18 15.3	4.78	145.43	33R	—	—	3.1	MAD		
13	15 09 07.6	4.94	144.98	66	—	—	3.4	MAD		
13	21 10 27.5	5.10	144.90	58	—	3.4	3.8	MAD		
13	23 55 40.2	4.87	145.61	33R	5.6	5.2	5.5	MAD		
*	23 55 39.7	4.88	145.62	32	—	—	5.1	*	25	76
14	01 59 32.3	5.04	145.27	65	—	—	3.7	MAD		
14	05 31 03.0	5.08	144.98	55	—	—	3.4	MAD		
14	09 34 00.3	4.98	145.78	33R	—	—	3.5	MAD		
14	18 59 52.7	4.94	145.19	77	—	—	3.4	MAD		
14	19 21 32.1	4.84	145.66	40	—	—	3.8	MAD		
14	21 09 35.1	5.08	145.29	33R	—	—	3.4	MAD		
15	00 57 58.5	4.86	145.07	104	—	3.6	4.1	MAD		
15	01 27 14.1	4.76	145.19	88	—	—	3.1	MAD		
15	02 27 28.7	5.01	145.20	33R	—	3.6	4.0	MAD		
15	06 25 00.9	5.11	145.16	56	—	—	3.4	MAD		
15	08 53 44.9	4.80	145.56	52	—	—	3.1	MAD		
15	10 13 05.9	4.75	145.86	37	—	—	3.4	MAD		
15	18 18 40.2	4.69	145.61	37	—	3.5	3.9	MAD		
16	07 57 07.0	4.82	145.63	49	—	—	3.4	MAD		
16	14 01 11.6	5.09	145.26	100	—	—	3.5	MAD		
16	18 43 14.3	4.87	145.18	93	—	—	3.1	MAD		
17	07 30 53.2	4.62	145.72	60	—	—	3.1	MAD		

TABLE 7. MADANG EARTHQUAKE SERIES — PMG AND (*) NOS DATA (*cont.*)

Date 1970	*Origin Time* UT	*Epicentre* Lat. °S	Long. °E	*Depth* km	*Magnitude* ML	MS	MB	*S-P* Stn	*No.* Stns	*EDR* No.
18	06 40 07.3	4.76	145.76	33R	—	—	3.1	MAD		
18	17 59 14.7	4.68	145.24	69	—	—	3.1	MAD, PLN		
18	20 40 00.7	4.71	145.86	33R	—	—	3.1	MAD, PLN		
18	21 12 15.9	4.74	145.29	43	—	—	3.4	MAD, PLN		
19	05 38 14.5	4.86	145.44	55	4.8	4.1	4.4	MAD		
19	07 39 25.2	4.79	145.74	4	—	3.7	3.8	MAD, PLN		
19	08 18 45.6	4.59	145.72	33R	—	3.6	3.6	MAD, PLN		
19	08 24 25.5	4.52	145.68	33R	—	—	3.1	MAD, PLN		
19	13 54 16.9	4.70	145.86	34	—	—	3.1	MAD, PLN		
19	15 10 17.9	4.61	145.97	33R	—	—	3.1	MAD, PLN		
19	23 59 58.5	5.01	145.19	65	—	—	3.1	MAD, PLN		
20	10 25 58.6	4.94	145.31	87	—	—	3.4	MAD, PLN		
20	13 00 57.0	4.94	145.17	80	—	—	3.1	MAD, PLN		
20	13 51 28.9	4.70	145.72	46	—	3.6	3.9	MAD		
20	15 39 41.7	4.79	145.25	83	—	4.1	3.8	MAD, PLN		
20	17 37 53.1	4.59	145.90	33R	—	—	3.4	MAD, PLN		
20	21 34 08.1	4.90	145.36	77	—	—	3.1	MAD, PLN		
21	05 03 47.8	4.80	145.68	46	—	—	3.4	MAD, PLN		
21	15 18 12.4	4.71	145.89	33R	—	—	3.1	MAD, PLN		
21	20 07 48.8	4.63	145.90	33R	—	—	3.4	MAD, PLN		
23	05 06 25.6	4.65	145.87	35	—	—	3.1	MAD, PLN		
23	06 34 02.1	4.55	145.75	33R	—	—	3.1	MAD, PLN		
23	11 15 29.6	4.93	145.39	82	—	—	3.1	MAD, PLN		
23	16 22 22.2	4.66	145.74	43	—	3.1	3.7	MAD, PLN		
24	05 54 49.6	4.43	145.90	33R	—	—	3.1	MAD, PLN		
24	17 30 01.2	4.98	145.16	35	—	—	3.9	PLN		
25	06 36 41.8	4.43	145.79	42	—	—	3.1	MAD		
25	16 33 36.2	(5.10)	(145.17)	(166)	4.7	4.6	4.6	MAD		
*	16 33 40.3	5.07	145.22	43	—	—	4.7	*	21	79
25	16 52 10.5	(4.59)	(145.32)	(95)	—	3.9	3.5	MAD		
25	18 47 21.8	4.94	145.26	80	—	—	3.4	MAD		
25	20 12 16.4	(4.81)	(145.46)	(148)	4.9	4.5	5.0	MAD		
*	20 12 21.8	4.92	145.64	34	—	—	4.3	*	14	81
25	20 18 57.2	(4.78)	(145.49)	(145)	4.4	3.9	4.4	MAD		

TABLE 7. MADANG EARTHQUAKE SERIES — PMG AND (*) NOS DATA (*cont.*)

Date 1970	*Origin Time* UT	*Epicentre* Lat. °S	Long. °E	*Depth* km	*Magnitude* ML	MS	MB	*S-P* Stn	*No.* Stns	*EDR* No.
*	20 19 02.3	4.92	145.65	33R	—	—	4.4	*	9	81
26	07 45 28.0	5.00	145.59	86	—	—	3.1	MAD		
26	07 54 32.0	4.94	145.54	80	—	3.9	3.8	MAD		
26	18 08 46.6	5.04	145.05	74	4.9	4.2	4.3	MAD		
27	12 58 07.2	4.54	145.78	41	—	—	3.5	MAD		
Dec.										
05*	09 52 34.1	4.94	145.61	51	—	—	4.9		26	80
19*	10 37 16.8	5.00	145.61	52	—	—	5.0		16	86
24*	13 11 15.9	4.86	145.62	57	—	—	4.6		16	87
1971										
Jan.										
01*	17 58 36.6	5.06	145.54	54	—	—	(4.6)		15	5
24*	13 50 06.3	5.16	145.91	156	—	—	(3.7)		9	13
Feb.										
01*	11 56 29.8	5.36	146.00	73	—	—	(4.2)		9	12
Apr.										
01*	06 56 05.1	5.10	145.18	60	—	—	4.6		11	26
12*	08 50 43.7	5.16	145.26	60	—	—	4.8		12	29
20*	00 07 07.9	4.85	145.75	36	—	—	5.1		26	29

* NOS data
(*) less accurate PMG value
33R restricted to normal depth

REFERENCES

THE PAPUA NEW GUINEA ADVISORY COMMITTEE ON SEISMOLOGY AND EARTHQUAKE ENGINEERING (ACSEE), 1973—Madang 1970 earthquake. *PNG Geol. Surv. Memoir* 2.

BAKER, S. H., 1970—Report on structural damage during an earthquake on 1 November 1970. *Report for the Administration of Papua & New Guinea, Department of Public Works* (unpubl.).

BERG, J. H., 1970—Report on earthquake damage in Madang and environs as a result of the earthquakes of 1 November 1970. *TPNG Commonwealth Department of Works Report* (unpubl.).

BOLT, B. A., 1965—The revision of earthquake epicentres, focal depths and origin times using a high-speed computer. *Geophys. J.*, 3, 433-40.

BROOKS, J. A., 1965—Earthquake activity and seismic risk in Papua and New Guinea. *Bur. Miner. Resour. Aust. Rep.* 74.

CHOUHAN, R. K. S., GAUR, V. K., & RATHOR, H. S., 1970—Aftershock sequence of the Solomon Islands earthquake of 15 June 1966. *Pure & app. Geophys.*, 80, 162-70.

CLIFTON-BASSETT, D., 1970—Report on the Madang earthquake. *Report for the Administration of Papua & New Guinea, Department of the Administrator* (unpubl.).

DENHAM, D., 1969—Distribution of earthquakes in the New Guinea-Solomon Islands region. *J. geophys. Res.*, 74, 4290-9.

DOW, D. B., SMIT, J. A. J., BAIN, J. H. C., & RYBURN, R. J., 1972—The geology of the south Sepik region, New Guinea. *Bur. Miner. Resour. Aust. Bull.* 133.

DUNCAN, B., & HOLLINGS, J. P., 1970—The Madang earthquake. *Report for the Administration of Papua & New Guinea, Department of Public Works* (unpubl.).

EVERINGHAM, I. B., 1973—The major Papua-New Guinea earthquakes near Madang (1970) and beneath the north Solomon Sea (1971). *Proc. 5th World Conf. Earthq. Eng.*, Rome, June 1973. (Also *Bur. Miner. Resour. Aust. Rec.* 1973/18, unpubl.)

EVERINGHAM, I. B., in prep. a—Preliminary catalogue of tsunamis for the New Guinea/Solomon Islands region. *Bur. Miner. Resour. Aust. Rep.* 180.

EVERINGHAM, I. B., in prep. b—Magnitudes of aftershocks of the 1970 Madang earthquake. *Bur. Miner. Resour. Aust. Rec.* (unpubl.).

HILL, R. H., 1970—Notes on the Madang earthquake, 1 November 1970. *CSIRO, Division of Building Research Report* (unpubl.).

HOGG, L., & ROBERTSON, S., 1971—The Madang earthquake: six weeks after. *Oceania*, 41, 298-311.

HOUTZ, R. E., 1962—The 1953 Suva earthquake and tsunami. *Bull. seismol. Soc. Amer.*, 52, 1-12.

JAMES, D. E., SACKS, I. S., LAZO, E. L., & APARICIO, P. G., 1969—On locating local earthquakes using small networks. *Bull. seismol. Soc. Amer.*, 59, 1201-12.

JOHNSON, T., & MOLNAR, P., 1972—Focal mechanisms and plate tectonics of the southwest Pacific. *J. geophys. Res.*, 77, 5000-32.

KRAUSE, D. C., 1965—Submarine geology north of New Guinea. *Bull. geol. Soc. Amer.*, 76, 27-42.

KRAUSE, D. C., 1972—Triple junction analysis and model studies of crustal plates in the Bismarck and Solomon Islands Seas. *Trans. Amer. geophys. Un.*, Abstr., 53, 412.

KRAUSE, D. C., WHITE, W. C., PIPER, D. J. W., & HEEZEN, B. C., 1970—Turbidity currents and cable breaks in the western New Britain Trench. *Bull. geol. Soc. Amer.*, 81, 2153-60.

LE PICHON, X., 1968—Sea floor spreading and continental drift. *J. geophys. Res.*, 73, 3661-97.

LILWALL, R. C., & UNDERWOOD, R., 1970—Seismic network bias maps. *Geophys. J.*, 20, 335-9.

MENARD, H. W., 1964—MARINE GEOLOGY OF THE PACIFIC. *International series in the Earth Sciences. New York, McGraw Hill.*

MOGI, K., 1968—Development of aftershock areas of great earthquakes. *Bull. Earthq. Res. Inst. Tokyo Univ.* 46, 175-203.

PAIN, C. F., 1972—Characteristics and geomorphic effects of earthquake initiated landslides in the Adelbert Range, Papua New Guinea. *Eng. Geol.*, 6, 261-74.

RICHTER, C. F., 1958—ELEMENTARY SEISMOLOGY. *San Francisco, W. H. Freeman.*

RIPPER, I. D., in press—Some earthquake focal mechanisms in the New Guinea/Solomon Islands region, 1963-1968. *Bur. Miner. Resour. Aust. Rep.* 178.

SIEBERG, A., 1910—Die Erdbebentätigkeit in Deutsch-Neuguinea (Kaiser-Wilhelmsland und Bismarck Archipel). *Petermanns Geographische Mitt.*, II Heft 2/3.

STODDART, D. R., 1972—Catastrophic damage to coral reef communities by earthquakes. *Nature,* 239, 51-2.

WYSS, M., 1973—Towards a physical understanding of the earthquake frequency distribution. *Geophys. J.*, 31, 341-59.